Progress in Polymer Science 35 (2010) 252–277

Contents lists available at ScienceDirect

Progress in Polymer Science

journal homepage: www.elsevier.com/locate/ppolysci

Biomolecular motors at the intersection of nanotechnology and polymer science

Ashutosh Agarwal [a], Henry Hess [b,*]

[a] Department of Materials Science and Engineering, University of Florida, Gainesville, FL 32611-6400, USA
[b] Department of Biomedical Engineering, Columbia University, New York, NY 10027, USA

ARTICLE INFO

Article history:
Received 2 September 2009
Received in revised form 9 October 2009
Accepted 22 October 2009
Available online 3 November 2009

Keywords:
Biopolymer
Hybrid device
Kinesin
Myosin
Microtubule
Actin
Molecular shuttle
Molecular motor
Motor protein
Cyotskeletal filament

ABSTRACT

The dynamic cytoskeletal components, biomolecular motors and their associated filaments, can be integrated *in vitro* with synthetic components to enable nanoscale transport systems. These "molecular shuttles" have generated significant scientific interest over the past decade, resulting in over 200 publications. This review focuses on the contributions involving the use of linear biomolecular motors, kinesin and myosin, and their associated filaments, microtubule and actin, in device applications. Exploiting the naturally occurring motion between the motors and their associated filaments requires an interdisciplinary understanding of the underlying challenges. Three basic topics that most of the experimental contributions have sought to address are: the guiding of shuttle movement, the loading and unloading of cargo onto the shuttles, and the control of motor activity. The physical properties of motors and filaments determine the engineering solutions to the design challenges. The applications, which center on the basic capability of nanoscale motion, and the roadblocks to their widespread implementation will be discussed in detail.

Contents

* Corresponding author. Tel.: +1 212 854 7749; fax: +1 212 854 8725.
E-mail address: hh2374@columbia.edu (H. Hess).

0079-6700/$ – see front matter © 2009 Elsevier Ltd. All rights reserved.
doi:10.1016/j.progpolymsci.2009.10.007

1. Introduction

Biomolecular motors, also known as motor proteins, are unique stimulus-responsive polymers. These particular amino acid polymers will undergo dramatic conformational changes as they bind and hydrolyze ATP and release the products in a cyclic process. Linear motors, such as myosin and kinesin, operate in conjunction with cytoskeletal filaments—actin filaments and microtubules, respectively. These filaments are linear polymers of thousands of actin or tubulin proteins and serve as the specific structures against which the motors exert forces. By coupling the conformational changes during ATP hydrolysis to changes in the motor affinity to the cytoskeletal filaments, motors can move along the filaments in a stepwise fashion.

A kinesin motor "walking" in a directed motion along a microtubule is a fascinating nanomachine (Fig. 1): about a thousand amino acids are arranged in a specific sequence that can fold into a structure with a "head" and a "tail". The head has an enzymatic site for the hydrolysis of ATP as well as a specific binding site for the attachment to the microtubule. The tail coils around the tail of a second kinesin monomer to create a two-legged structure that also acts as a connector to bind and move specific cargoes. The hydrolysis of each ATP molecule causes a precise sequence of conformational and affinity changes which is coordinated between the two heads of each kinesin dimer. The energetic efficiency of this process can exceed 50%, making it higher than the efficiency of a car engine [1,2].

Biomolecular motors, and in particular kinesin, are thus a prime example how polymeric structures have evolved in nature with a performance unmatched by any man-made polymer. These motors are truly nanomachines, which have tamed thermal fluctuations so that an individual molecule can predictably perform a sequence of hundreds of steps. Clearly, the behavior of these polymers is not discussed in a textbook of equilibrium thermodynamics.

It is instructive to compare biomolecular motors to synthetic stimulus-responsive polymers, such as poly(N isopropyl acrylamide) (PNIPAM). While PNIPAM is often utilized in gels with macroscopic dimensions [3–6], or thin films [7,8], its stimulus response can also be exploited on the molecular scale. For example, individual molecules of PNIPAM can be grafted onto proteins [9,10] where their phase transition from a collapsed to an extended conformation is exploited to block a binding site. However, to actuate the PNIPAM molecule, the stimulus has to be externally applied to the entire environment of the molecule. In contrast, a biomolecular motor operates

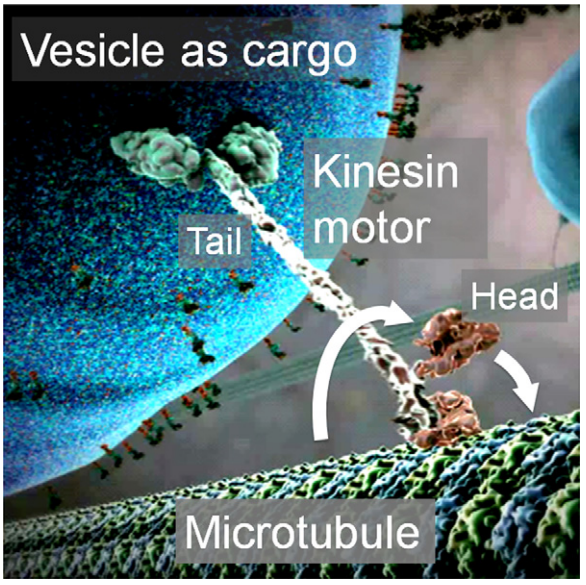

Fig. 1. The kinesin-1 motor protein transports cargo, such as vesicles, along the microtubules inside a cell. Kinesin is a dimer, where each amino acid chain folds into a head (the ATP-hydrolyzing and microtubule-binding motor domain) and a tail domain. The two tails form a coiled coil, which holds the two subunits together. The coordinated movement of the two heads enables a "walking" motion. Still image from the animation "The Inner life of the cell", a collaboration between Harvard University and XVIVO, LLC. Reproduced with permission by Alain Viel and Robert A. Lue, Harvard University. Copyright 2007 The Presidents and Fellows of Harvard College.

autonomously in a constant environment. While some artificially designed DNA motors [11,12] have recently been able to achieve autonomous operation, their speed and efficiency are orders of magnitude lower than those of biomolecular motors.

The performance advantages of biomolecular motors over synthetic stimulus-responsive polymers are maintained if the motors are integrated into macroscopic structures, such as a muscle. A muscle, e.g. a biceps, contains on the order of $10\hat{2}0$ myosin motors coupled together into a macroscopic structure, but it still achieves a maximal efficiency exceeding 20% [13]. In contrast, the efficiency of energy conversion in a PNIPAM gel has been estimated as 0.001% [5].

Beyond evolving a highly functional molecular motor, nature has accomplished other feats of interest to the polymer chemist, materials scientist or nanoengineer: myosin motors have been hierarchically assembled over multiple length scales into muscle, which is an accomplishment unmatched by any synthetic polymer system. Control of motor activity has been achieved on the macroscale via the neuromuscular system, as well as on the subcellular scale via a variety of molecular mechanisms [14,15]. Motors and cytoskeletal filaments combine into a multifunctional, adaptive material [16,17]. Last but not least, applications have been found for molecular motors, derived systems, and materials.

Biomolecular motors have attracted tremendous interest from physiologists, biologists and biophysicists due to their central role in the musculoskeletal system. Tens of thousands of publications describe biomolecular motors from the perspective of the natural sciences and biomedicine.

This review, in contrast, will describe an engineering frontier, which has emerged in the past ten years: the design of hybrid systems incorporating biomolecular motors. The focus of this effort is in the realm of nanotechnology because providing actuation at the nanoscale is particularly challenging by other means, and because a functional nanosystem requires fewer molecular scale parts than a system on the meso- or macroscale. The importance of polymer science concepts will be highlighted, since they are encountered at two scales: the molecular scale of individual motor proteins and the supramolecular scale of cytoskeletal filaments, which can be thought of as "polymers of polymers". Systems designed from linear motors are emphasized here, since the efforts in the utilization of the rotary motor F1-ATPase [18–20] have slowed, due to the difficulty of utilizing this protein in a synthetic environment.

This review is the latest of a series of efforts to summarize the state-of-the-art in the field [21–33], and aims to be an up-to-date and comprehensive overview. The organization of the manuscript is as follows: after an introduction to the basic properties of cytoskeletal filaments and the motor proteins myosin II and kinesin-1, we will focus on the design of nanoscale transport systems powered by kinesin and myosin and review the extensive research concerning these systems. We will conclude with a review of the applications which have been described and a brief outlook into the future.

2. Cytoskeletal filaments

The cytoskeleton consists of a network of actin filaments, microtubules and intermediate filaments [34]. This protein scaffold assists the eukaryotic cell in organizing its cytoplasm, in responding to external mechanical stimuli, and in generating motility [35,36].

Actin, one of the most abundant proteins in eukaryotic cells [37], plays both dynamic and structural roles [38]. Along with actin-binding proteins (ABPs), the actin cytoskeleton provides mechanical strength to the cell, connects transmembrane proteins with cytoplasmic proteins, and generates locomotion in cells [39].

Microtubules are long, stiff, and hollow biopolymers found in all eukaryotes [40]. They nucleate at and grow out from microtubule-organizing centers such as centrosomes [41], span the entire cytoplasm, and provide structural support to the cell [42]. Together with microtubule-associated proteins (MAPs), these remarkable constructs are involved in a variety of cellular functions such as intracellular transport, cell motility, and mitosis [35].

Intermediate filaments are ropelike polymers composed of tetramerized alpha-helical rods with N- and C-terminal domains. The structure and function of intermediate filaments depend on their intracellular location [43]. For example, lamin provides stability to the nuclear membrane, vimentin withstands stresses in the cytoplasm of the cell, and desmin provides linkages within muscle fibers.

Since microtubules and actin filaments also serve as tracks for motor proteins, their structural organization will be reviewed in more detail.

2.1. Actin filaments

Actin monomers called G-actin (globular-actin) polymerize in the presence of ATP and millimolar concentrations of Ca^{2+} or Mg^{2+} to form right-handed, double-stranded helical filaments. These filaments, called F-actin (filamentous-actin) have a diameter of 8 nm [38] and consist of two strands which cross over every 36 nm, giving a full 360° turn every 72 nm [44]. The monomers incorporate into the filament in a specific orientation, thus imparting a structural and functional polarity to the filament. Based on their appearance in electron microscopy images, when coated with myosin motor domains (myosin subfragment 1), the fast-growing end is designated as the "barbed end", while the slow growing end is referred to as the "pointed end" of the filament. Motor proteins of the myosin family bind to actin filaments and, generally, move in the direction of the barbed end. *In vivo*, actin filaments are very dynamic structures which are in a dynamic equilibrium between polymerization and depolymerization. *In vitro* however, actin filaments can be stabilized against depolymerization with phalloidin [45]. This stabilization is essential for their use in engineered structures.

The wire-like actin filaments with a trajectory persistence length of less than 10 μm [46–48] are employed in hybrid devices if myosin motors are preferred or particularly flexible filaments are desired.

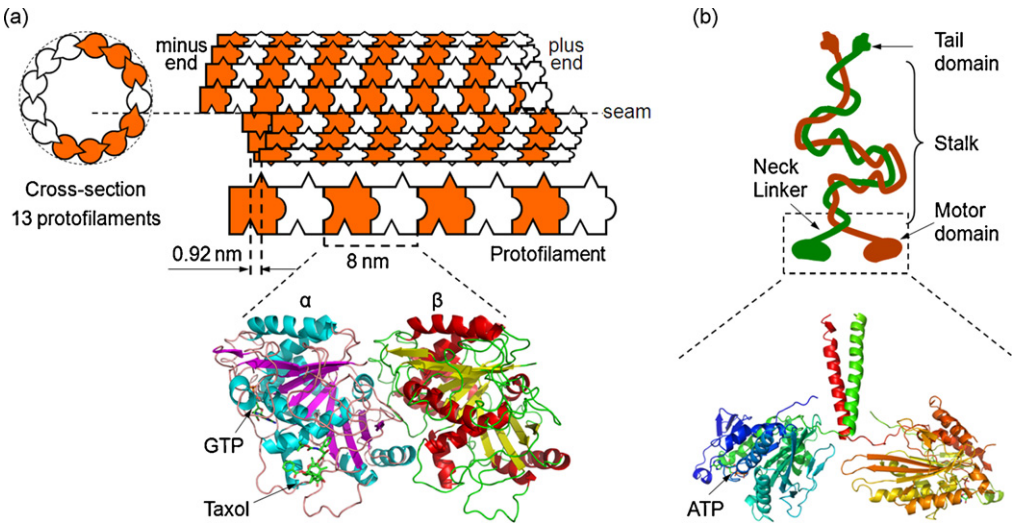

Fig. 2. (a) Schematic representation of a microtubule with 13 protofilaments. Protofilaments are made from tubulin dimers which bind to each other in a head-to-tail fashion. Protofilaments bind to each other with an offset which results in a seam in the microtubule structure. The ribbon diagram (bottom) is derived from electron crystallography [49] and shows the GTP and taxol binding sites. (b) Schematic representation of kinesin showing the cargo binding tail domain, the coiled coil stalk domain, the neck linker, and the head domain of the molecule. The ribbon diagram is derived from X-ray crystallography [50] and shows the ATP binding site in the head domain.

2.2. Microtubules

Microtubules are hollow cylinders composed of α,β-tubulin heterodimers [51]. Tubulin dimers bind head-to-tail to form linear protofilaments with an 8 nm repeat distance and a variable number (10–18, often 13) of protofilaments and assemble into a cylindrical structure with an outer diameter of about 25 nm and a length of many micrometers (Fig. 2a) [52]. Since the protofilaments bind to each other in the same orientation, the microtubule also develops structural polarity. The end exposing α-tubulin is slow-growing and called the minus end, and the fast-growing end exposing β-tubulin is named the plus end. However, protofilaments bind to each other with an offset of 0.92 nm, which results in an accumulated offset of 12 nm from 13 protofilaments. This exactly equals the length of three monomers and hence, for a 13 protofilament microtubule, a discontinuity in the structure or a linear 'seam' exists. The structural properties of microtubules are critical to their cellular functions as well as their nanotechnological applications.

During polymerization, microtubules can display a phenomenon termed dynamic instability: stochastic switching between growing and shrinking phases on a timescale of minutes [53]. When microtubules are in a growth phase, the tubulin dimers joining the plus end have a GTP molecule bound to them, which they subsequently hydrolyze to GDP [54]. If polymerization proceeds faster than hydrolysis, a "cap" of GTP-tubulins is formed at the microtubule tip, which stabilizes the microtubule. If hydrolysis overtakes polymerization, the GTP cap is destroyed and rapid depolymerization sets in (a phenomenon known as "catastrophe"). The depolymerization of the microtubule stops when a surviving GTP tubulin is encountered in the microtubule lattice, which arrests the depolymerization and initiates a new growth phase (the process is termed "rescue") [55]. Hence, microtubule assembly depends critically on the binding, hydrolysis, and exchange of the nucleotide GTP [56], which acts by changing the conformation of the tubulin dimer [57].

Dynamic instability enables cells to perform multiple tasks. Regulated assembly and disassembly of microtubules can generate pulling and pushing forces [58], and is used by cells to position the mitotic spindle and separate the two sets of chromosomes into the two daughter cells [59,60]. Dynamic instability also allows cells to recycle the tubulin building blocks. From a materials perspective, constantly turning over the subunits of a structural element might also allow cells to ensure that these components remain defect free [61].

The diversity of tasks that cells are able to fulfill by controlling dynamic instability has piqued the imagination of nanotechnologists too. Simulations have shown that the seemingly unreliable stochastic process of dynamic assembly can be employed to build a variety of nanostructures [62]. Strategies to sort, pattern, harvest, and deliver nanoparticles have been evaluated (Fig. 3a). Reproducible control over the actions of these nanosystems can be exercised only at the "swarm" level, where the stochastic nature of individual elements is averaged [62,67]. The initial steps towards an experimental demonstration of these concepts have been taken by assembling three-dimensional polar-oriented synthetic microtubule organizing centers [68].

The reversibility of the actin or tubulin polymerization is also employed for the preparation and purification of proteins functionalized with fluorophores or biotin, for example [69,70]. It is essential that the ability of the protein to polymerize is not compromised after functionalization. Hence, microtubules are labeled in the polymer form, excess label is removed and functional protein is selected by repeated cycles of polymerization, centrifugation and depolymerization. Nanoparticle-labeled actin monomers

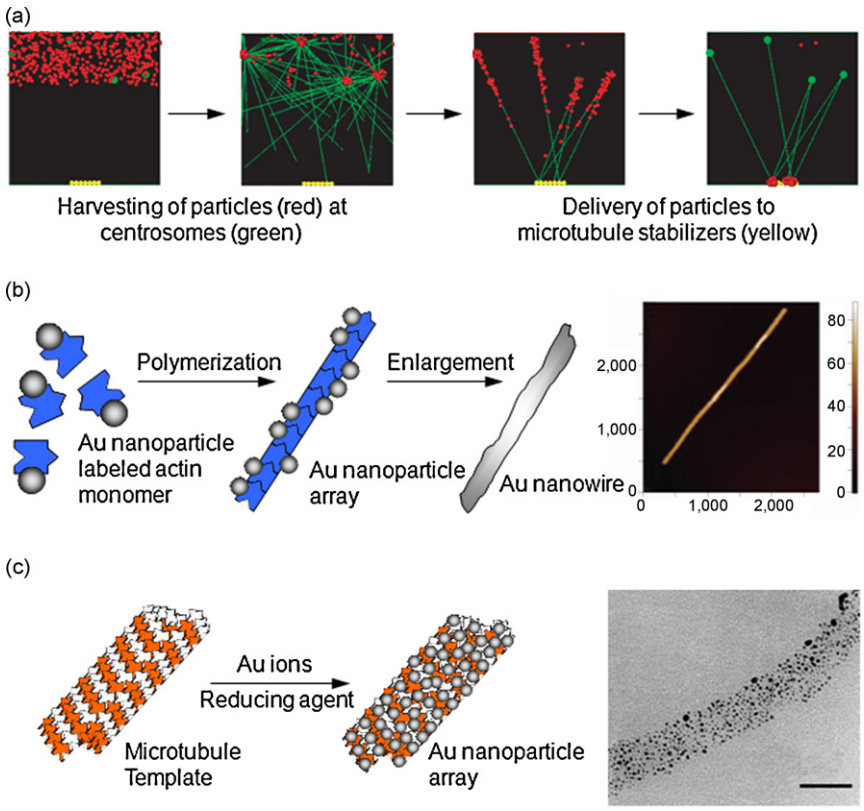

Fig. 3. Nanotechnological applications derived from filament properties. (a) Snapshots from a simulation study [62] which illustrates the harvesting of nanoparticles by microtubules and the delivery of harvested particles to defined locations. The harvesting process and formation of stable tracks to the destination location employs dynamic instability. Figure adapted with permission from Bouchard et al. [62]. Copyright 2006 by the American Physical Society. (b) Fabrication of gold nanowires using actin filaments as templates via polymerization of gold-labeled actin monomers and subsequent metallization [63]. The AFM image of a gold nanowire obtained by this procedure is reproduced from [63]. Reprinted by permission from Macmillan Publishers Ltd.: Nature Materials [63], Copyright 2004. (c) Microtubules have been used as templates to nucleate and grow nanoparticles from metal ion solutions in presence of reducing agents [64–66]. The transmission electron microscopy image shows a microtubule densely covered by gold nanoparticles; the scale bar represents 100 nm. TEM image is reproduced from Behrens et al. [66]. Copyright Wiley-VCH Verlag GmbH & Co. KGaA. Reproduced with permission.

have also been successfully prepared by this process and subsequently been polymerized [63]. The resulting filaments have been subjected to catalytic enlargement of the gold-nanoparticles to generate continuous gold nanowires (Fig. 3b). Fluorescently labeled tubulin and biotinylated tubulin have also been prepared and are commercially available in lyophilized form in ready-to-use aliquots (Cytoskeleton Inc., Denver, CO, USA).

Frequently, a static microtubule structure is desirable. To this end, depolymerization can be suppressed for days by the addition of paclitaxel (taxol) to the buffer solution [71]. Microtubules can also be chemically cross-linked using glutaraldehyde. This extends their lifetime to weeks and makes them stable at temperatures as high as 90 °C and against large variations in pH [72,73].

Due to their nanoscale cross-section, very high aspect ratio, and well-ordered surface functionality, stabilized microtubules can be used as templates for the production of inorganic nanowires [65,66,74] and nanoparticle arrays (Fig. 3c) [64,66]. Iron oxide-coated microtubules [74] have been produced by a biomimetic mineralization process with a fair amount of control over the oxide thickness and crystallinity. Tubulin–carbon nanotube hybrids, including microtubule encapsulated-nanotubes have also been reported [75].

3. Biomolecular motors

Cells contain a wide variety of biomolecular motors, including the F1-ATPase rotary motor [76], DNA polymerase [31] and the motor proteins of the myosin, kinesin and dynein families [77]. All of these motors can utilize chemical energy to generate mechanical motion. Kinesin-1 (conventional kinesin) and myosin II (muscle myosin) are of particular utility in nanotechnology, because their primary function is the exertion of force, and they will be discussed in some detail in the following two sections. Dynein motors have not been traditionally employed for nanotechnological applications; hence their detailed discussion is omitted. While myosin moves along actin filaments, kinesin and dynein walk along microtubules. The key to the generation of motion by motor proteins is a conformational change in the globular 'head' domain of the motor as a result from adenosine triphopsphate (ATP) hydrolysis while the head is attached to the associated filament. The conformational change is amplified and results

in movement of the load bearing 'tail' region of the motor in a specific direction along the filament. The amplification is provided by the lever arm 'neck' domain and depends directly on the length of this lever arm [78]. After this 'power stroke', the head detaches, advances and rebinds at the next binding site on the filament. The fraction of time that each head spends in its attached state is called the duty ratio of the motor. Differences in the duty ratio are important in determining if the motors are processive or not [34]. A non-processive motor detaches from the filament after every step while a processive motor stays attached for multiple steps. Motors have evolved with different duty ratios to serve distinctly different cellular functions [34]. For example, highly processive kinesin motors are utilized individually by cells for long distance intracellular transport, while non-processive myosins are used in parallel in large numbers to produce rapid motion.

3.1. Myosin

Myosin motors are involved in intracellular organelle transport [79], cell movement [80], endocytosis and exocytosis [81,82], and mechanotransduction [83]. Most importantly, myosin movement along actin filaments is the force-generating mechanism for muscle contraction [84–86].

From the myosin family (myosin I–XXIV [87]), primarily myosin II has been chosen for engineering applications due to its wide availability [28], although myosin V has been employed as well [88]. The non-processive myosin II (duty ratio of about 0.05 [89]) works in large arrays in muscle fibers where each motor contributes a small and quick translocation of the associated actin filament. The processive myosin V (duty ratio of 0.7 [90]) is employed for long-distance intracellular cargo transport. The kinetic mechanism of myosins has been modeled as a power-stroke model [91] and less frequently as a biased Brownian ratchet [92,93]. The *in vitro* speed of purified myosin II motors at saturating ATP concentrations is about 6 μm/s, and each motor generates a force on the order of 1 pN [34].

3.2. Kinesin

Kinesin-1 motors are primarily involved in intracellular transport of vesicles and organelles [95]. Their role becomes particularly important in neurons because vital cargo has to be transported over large distances [96]. Kinesins are also involved in cell division [97], and the organization of cilia and flagella [98].

Kinesin-1 is a two-headed motor which walks towards the plus end of the microtubules (Fig. 2b). It is a tetramer of two identical "heavy chains", and two associated light chains, which *in vivo* are responsible for cargo binding. The heavy chains fold into two globular heads at one end, a stalk with a hinge in the middle, and a tail domain at the other end [99]. The heads step on the binding sites along the microtubule protofilaments. These sites are spaced 8 nm apart. Each head of the kinesin molecule takes 16 nm steps, thus moving the entire molecule 8 nm in each step in a hand-over-hand mechanism [100]. The heads pass each other on alternating sides to keep the stalk from getting twisted during the walk. For every step, kinesin consumes one ATP molecule [101]. The two heads are tightly coordinated so that one head does not detach before the other is securely attached. This makes kinesin a highly processive motor [102], allowing it to walk for several micrometers before detaching. The exact sequence of events in the mechanochemical cycle of kinesin is still debated but one possible description is depicted in Fig. 4 [94]: the tail domain, if not bound to the cargo, inhibits motor activity by binding to the motor region, presumably to conserve ATP and maintain the kinesin position near the cargo loading area [103].

In vitro, kinesin motors walk along microtubules at speeds of 1 μm/s (saturating ATP concentrations [34]). The force at which the mean velocity drops to zero, the stall force, is about 8 pN and is independent of ATP concentration [34]. Because of its high degree of processivity, even a single kinesin molecule is capable of propelling microtubules along a surface [104].

4. From motility assays to nanoscale transport systems

Biophysicists have for a long time utilized *in vitro* assays to study motor proteins and their associated cytoskeletal filaments in a synthetic environment [105–108]. These "motility assays" enable the purification and identification of the involved biological components, the controlled arrangement of biological and synthetic structures, and the sensitive detection of the ensuing events. Motility assays have been conducted in the "bead geometry" (filaments stationary, motors moving) and in the "gliding geometry" (filaments moving, motors stationary). Both approaches have been adopted by engineers aiming to mimic the biological applications of motor proteins, and in particular their function as nanoscale transport systems. These nanotransporters are often referred to as "molecular shuttles".

4.1. Bead geometry

In the bead geometry, the cytoskeletal filament – often a microtubule – is immobilized by adsorption to a surface while the motor is attached to a polystyrene microsphere (the "bead") and walks along the filament. Optical tweezers can be used to exert precisely calibrated opposing forces on the bead and consequently on the motor. The displacement of the bead as a function of time reveals the individual steps of the motor heads. These data helped unravel the walking mechanism of molecular motors [109–116]. Fusion proteins combining a motor with a fluorescent protein enable the imaging of motor movement with even less interference, albeit without the ability to exert a defined load.

For processive motors such as kinesin, dynein, and myosin V, the associated filament is fixed to a slide surface while the motor protein is fixed to the trapped bead through its tail (Fig. 5a). The trap can now either remain stationary and exert increasing forces as the motor moves on the filament, or serve as a 'constant force clamp' [117] through a feed-back loop that moves the laser focus. Multiple motors of the same [118] or different [119] kind can also be attached to the same bead to model the transport

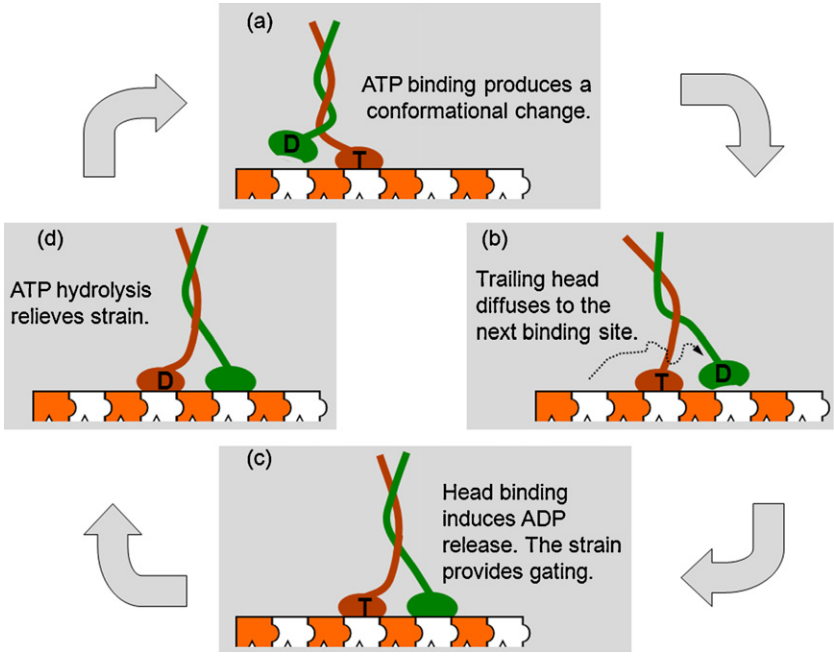

Fig. 4. Asymmetric hand-over-hand mechanochemical cycle of kinesin [94]. (a) ATP binding to the leading head induces a conformational change in the molecule. This power stroke results in the movement of the trailing head towards the plus end of the microtubule. (b) The trailing head reaches the next binding site, 16 nm away on the microtubule lattice, after a diffusional substep. (c) Binding to the microtubule catalyzes ADP release from the new leading head. This strains the neck linker region which gates the two head domains in different states. (d) ATP hydrolysis and release of phosphate from the now trailing head relieves the strain, freeing the leading head to bind to an ATP molecule to repeat the cycle.

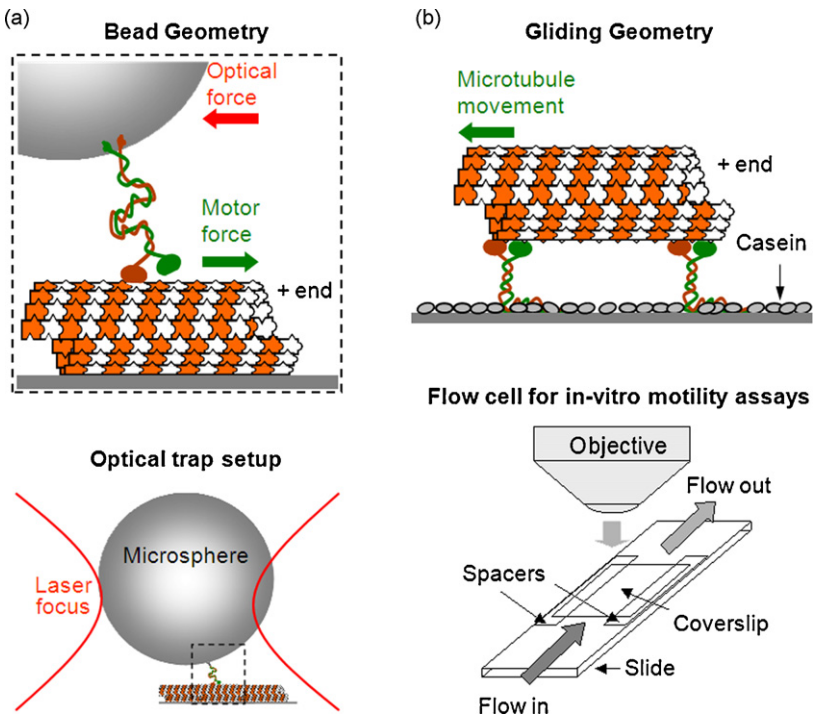

Fig. 5. Design routes for nanotechnological applications. (a) Bead geometry. This is most often employed in an optical tweezer setup utilized by motor biophysicists. Filaments adsorbed to a substrate serve as tracks for motors. Microsphere cargo is bound to the tail region of the motors and held in place by a laser trap. (b) Gliding or inverted geometry. Motors are adsorbed to a substrate through their tail domains. The heads project out into the solution and bind to filaments. The experiments are usually carried out in a "flow" cell which enables solution exchanges (but does not utilize continuous flow) and investigation under a microscope.

properties of cargo being propelled by several motors; a situation much closer to the complex traffic inside the cell.

For non-processive motors such as myosin II, the optical trap setup is usually modified [113,120]. Beads are attached to the coverslip to provide docking of the motors via their tails. A filament is stretched between two beads via double optical tweezers and brought close to the coverslip surface to interact with one or more motors. A recent review summarizes the use of optical tweezers in the study of non-processive motors [121].

The distance over which the bead is transported depends on the number of motors connecting the filament and the bead [118], but can only exceed the length of the filament if the immobilized filaments are overlapping [122].

4.2. Gliding geometry

The gliding geometry (or "inverted geometry") utilizes immobilized motors and a moving filament. This is advantageous as the filament can move for centimeters without interruption, provided a sufficient area has been covered with motors. Furthermore even non-processive motors, such as myosin II, can transport filaments over long distances since a large number of motors can simultaneously interact with the filament [92]. Gliding assays are typically performed in simple 'flow cells' assembled from a glass slide and a glass coverslip separated by spacers of roughly 100 μm height (Fig. 5b) [108].

The interaction between the motors and the internal surface of the flow cell in a gliding assay has been shown to be critical [29,30]. The direct binding of a motor to the glass surface of the coverslip leads typically to denaturation of the motor protein with a complete (neither filament binding nor transport) or partial (binding but not transport) loss of function of the motor. Coating the surface with a nitrocellulose film (for myosin) or a blocking protein such as casein (for kinesin, Fig. 5b) has been shown to dramatically enhance the motor activity after non-specific adsorption [108,123]. In addition, strategies to specifically adsorb motors to coatings on the surface have been explored [124,125].

The gliding of filaments can be imaged by dark-field, differential interference contrast, or fluorescence microscopy. While the filaments appear significantly wider than they actually are due to the resolution limitations of optical microscopy, the position of isolated filaments can be determined with nanometer accuracy in three dimensions [126,127]. For example, it has been established using fluorescence interference contrast microscopy that kinesin holds the microtubule 17 nm away from the surface [128].

4.3. Nanoscale transport by molecular shuttles

While bead and gliding assays reconstitute some aspects of *in vivo* motor functions, they are far from recreating the motor-based transport system of a eukaryotic cell. In the gel-like cytoplasm of these cells, a rich variety of motor proteins has evolved to transport specific organelles and vesicles over large distances from one defined location to another at controlled rates and well-defined points in times [129].

To mimic the biological transport system, the functionality of the bead or gliding assay would have to be significantly expanded. By integrating directed transport along predefined paths, loading and unloading of specific cargoes and user-controlled activation of the motors a fully functional biomimetic nanoscale transport system could be created. Such a system, termed "molecular shuttle" [130,131], was envisioned to serve as a component of miniaturized devices and functional materials.

In the context of miniaturized devices [132], the critical advantage that motors confer is that there is no need of external pumps to power the mass transport functions. The chemical energy derived from ATP molecules, present within the system, is directly harnessed to generate motion. Active transport by molecular shuttles also complements diffusion, pressure-driven flow or electrokinetic transport in micro and nanofluidic devices since its effectiveness scales differently with the transport distance [21,23,133].

Molecular shuttle designs can be based on either the bead or the gliding assay (Fig. 5), with each configuration offering distinct advantages.

Control over direction of motion is most elegantly achieved in the gliding assay. Due to the intrinsic structural polarity of the filaments, the resulting motion in a gliding assay is always towards one end of the filament. The gliding filaments can be guided in a specific direction by a variety of techniques, which are discussed in the next section. For directional control in bead assays, oriented filaments have to be immobilized on the surface in high densities. Immobilization has been achieved through silane–microtubule interactions [134,135], minus end-specific antibodies [136], immobilizing seeds on the surface [137], selective DNA hybridization [138], or using modified motors that only bind to filaments [139]. Subsequent alignment is achieved through fluid flow [134–136] or elongation of the immobilized filaments through polymerization [137,139]. However in the majority of studies, filaments are first aligned using the gliding assay and then immobilized to serve as tracks for motor coated beads.

In the gliding assay, diverse cargoes can be attached in high density to filaments by conventional bioconjugation techniques [69]. As discussed earlier, the actin or tubulin subunits are typically first functionalized and purified, and then reassembled into filaments with the desired properties. In a bead assay, however, apart from generating dense tracks of oriented filament, functional motors need to be adsorbed in high density to the cargo surface [118].

The basic challenges of guiding the movement, loading the cargo, and controlling the motors are common to all molecular shuttle systems, and are reviewed in the following sections. However, since the bead geometry has only been employed in a few instances [122,140–148], the discussion will focus on systems utilizing the gliding geometry.

5. Guiding molecular shuttles

On planar surfaces uniformly coated with myosin or kinesin motors, actin filaments and microtubules, respectively, perform persistent random walks [47,149]. These

paths result from the Brownian motion of the filament tip, which searches for the next motor as the advancing filament is anchored to the preceding motors. The emerging trajectory thus can be modeled as a worm-like chain, whose stochastic properties – just as the polymeric filament itself – can be characterized by a persistence length.

While some device designs can take advantage of the random movement of shuttles [132,150], in most cases it is essential to guide molecular shuttles along predetermined paths. In addition, it is desirable to define a specific direction of transport along the path as well as to have the ability to switch between alternative paths.

The approaches that have been used to design guiding tracks are: (1) physically erecting steep side walls for channels that guide shuttles moving on the bottom surface, (2) chemically defining track regions where motor proteins are adsorbed and surrounded by non-track regions so that shuttle motility is restricted within track regions, (3) combination of both these techniques, where only the channel bottoms have functional motor proteins and walls do not have active motors, and active steering of shuttles using (4) flow fields, (5) electric fields and (6) magnetic fields.

5.1. Guiding using surface topography

Surface topography provides physical confinement by imposing barriers to filament motility. When the shuttles collide with the walls of the barriers, the propelling force of motor proteins is transformed into bending forces for the filaments. This results in guiding along the direction of channel walls (Fig. 6a) [151,152].

The first physical guiding design for both the actomyosin system [153] and the kinesin–microtubule system [130] were simple ridges and grooves along the shear axis of a mechanically deposited PTFE film on glass. The widths and heights of ridges however, were difficult to control. Replica-molding of polyurethane channel reproducibly produces channel geometries [131]. While these open guiding channels have to be sufficiently deep (>200 nm) to prevent the microtubule or actin filament from climbing the wall [127,154], the angle of approach is also a key determinant of the outcome of filament-sidewall collisions (either guiding or escape) and hence of guiding efficiency [155].

The adsorption of filaments to the guiding channels in random directions leads to bidirectional movement of shuttles along the tracks. Extraction of unidirectional movement was made possible by adding 'arrowhead'-shaped rectifiers to the tracks [156]. While these rectifiers selected the direction of movement with a 70% success rate, several advanced rectifier designs have now been tested for rectification efficiency and analyzed for the rectification mechanism [157,158]. A more detailed understanding of filament gliding trajectories [149] has also enabled simulations aiding the design of tracks for systems based on microtubules [159] and actin filaments [47].

Another design advance was the introduction of an undercut at the bottom of the channel wall [160] (Fig. 6b). Microtubules [160] and actin filaments [161] are unable to climb the sidewall and hence preferentially move in the undercut section of the channel. These undercuts were later combined with other rectifier designs [122,162] for efficient guiding and generation of unidirectional motion.

Completely enclosed microfluidic channels have also been employed for kinesin–microtubule shuttles [163]. While open channels have to guard against the escape of filaments, these capped channels inherently provide three-dimensional confinement. Directional rectifiers have been

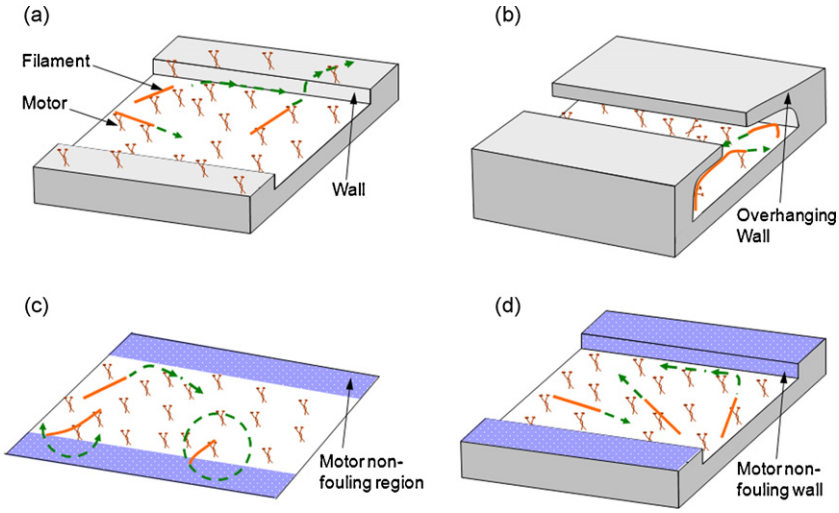

Fig. 6. Guiding approaches. (a) Guiding using surface topography. The normal force provided by the walls to the motor propelled filaments bends them along the wall. However, a fraction of the filaments, depending on the approach angle, are able to climb the walls and escape due the availability of motors on the walls. (b) Guiding in the presence of an undercut just below the wall. Filaments that climb the wall are redirected back into the region between the channels. (c) Guiding using surface chemistry by generating sufficient contrasts in motor functionality between two regions. When filaments cross the track edge an overhanging tip emerges, which fluctuates under the influence of thermal forces until it binds to a motor in the motor-rich region. A filament bound to a last motor can rotate more freely because motors can swivel around their axis. (d) Guiding using surface topography and chemistry. The surface chemistry of the walls is designed to interfere with either binding or functionality of motors. Filaments are redirected along the walls for steep and small approach angles, resulting in superior guiding as compared to surface topography alone or surface chemistry alone approaches.

incorporated into closed channels [164] and the use of electrical fields in closed channels has even enabled dynamic control of the filament path [165].

Directional control in bead assays involves laying down filaments in an isopolar orientation, which has been achieved using the gliding assay. Rectifiers with built-in overhangs were employed in one study [122] to orient kinesin-propelled short microtubule seeds. Seeds were immobilized and extended by polymerization into oriented networks of microtubules. The oriented microtubule tracks were then shown to support the motility of kinesin-coated nanospheres with a strong directional preference. In an alternative approach [144], surface patterns were used to position individual microtubules which were then immobilized by UV light to serve as tracks in the bead assays.

5.2. Guiding using surface chemistry

An alternative to physical barriers that force the filament into the desired direction are patterns in motor density and/or functionality, which bias the Brownian motion of the filament tip in the direction of the track (Fig. 6c). When a filament moving on a track reaches the boundary of a region which is either free of motors or contains inactive motors, an overhanging filament tip not bound to any motors emerges. This tip either keeps growing in length until it detaches completely from the surface or it bends back to the motor-rich area as a result of its Brownian motion. It has an increased chance of returning to the motor-rich area when it is held only by the very last motor, because it can swivel around the motor axis [166]. A small angle of approach of the filament to the boundary and low filament stiffness facilitate the return of the filament tip to the track [151,152].

Patterns in motor density or functionality can be created by patterns in the surface chemistry supporting the layer of motor proteins. This approach was first demonstrated in actomyosin systems by fabricating various patterns of tracks of hydrophobic PMMA on a hydrophilic coverslip by photolithography [167]. In the next report, the hydrophobicity of a copolymer film of *tert*-butyl-methacrylate (*t*BuMA) and methyl methacrylate (MMA) was modulated using e-beam irradiation. Actin motility remained confined within the narrow hydrophobic lines corresponding to the unexposed regions of the polymer film [168]. Testing of several materials revealed that a trimethylchlorosilane (TMCS) surface, produced by silanization, is a good substrate for myosin binding in the *in vitro* motility assay [169]. TMCS/silica micro patterns and nanopatterns were created using UV lithography and e-beam lithography respectively [170]. Different modes of myosin adsorption on different surfaces have been identified [171].

Producing contrasts in both, kinesin density and functionality, is more challenging because the frequently employed casein layer partially shields kinesin from the surface. As a result, microtubule motility is supported on a wide variety of surfaces. Non-fouling coatings offer a solution, since they suppress the adsorption of both casein and kinesin [151,172].

Motor adsorption can also be mediated through specific interactions. For example, patterns of streptavidin have been generated on gold-coated substrates using dippen lithography and microcontact printing. Biotinylated myosin has then been attached onto these while albumin has been utilized to avoid non-specific adsorption [173]. Biotinylated kinesin has also been used to achieve directed attachment [174]. Nanometer-scale gold lines within the walls of micrometer-sized chambers have been used to generate biotin-derivatized SAMs. Biotinylated kinesin has been attached to these SAMs via streptavidin and intermediate layers of biotinylated albumin. Microtubule sliding is thus confined to these tracks on the walls of the chamber. Patterns of carbon nanotube networks have also been shown to be effective barriers to myosin adsorption and hence the spatial activity of actomyosin [175].

Nanometer-wide tracks of myosin [176] and kinesin [177] have been generated by a biotemplated stamping technique. The filament lattice itself was used as a stamp to bind and transfer motor proteins to planar surfaces. The deposited motors then released the template filament, leaving behind nanometer wide tracks of motors able to bind and propel filaments in either direction along the track.

5.3. Guiding using surface topography and chemistry

Problems with both surface topography and chemical guiding approaches have been already recognized in early reports [131,168]. In topographical confinement, filaments can climb the sidewall (due to motors being present there) and escape [131]. When chemically confined, filaments crossing the boundary may detach from the surface, because their motion is not redirected by a wall [168]. The probability of filament loss in both cases depends primarily on the angle of approach to the boundary and the filament stiffness [151]. The logical solution to these problems is to combine both approaches and confine motor adsorption/functionality only to the bottom surface of the guiding channel. For the kinesin–microtubule system, this combination has been achieved by constructing polymer channels with non-fouling on a glass surface. For the actomyosin system, a variety of different resist materials with inherently different or modifiable hydrophilic character have been employed.

In the first demonstration of guiding by non-fouling topographical features [156], Triton X-100, a non-ionic detergent, has been used to render channel walls non-fouling. The study was also the first to introduce the use of direction rectifiers within guiding channels to extract unidirectional shuttle movement. Since then, non-fouling channel walls have been generated by physisorbing Pluronic F108 to hydrophobic SU-8 walls [151] and to polymer walls rendered hydrophobic by fluorosilanes [178]. In a later study [179], it was proven that SU-8 photoresist by itself also does not support kinesin-based motility and can be used to effectively guide shuttles [180]. Motility has also been achieved on gold patterns etched into a SiO_2 surface which was later functionalized with poly(ethylene glycol) chains [181,182].

Combined guiding approaches for the actomyosin system started with the use of laser ablation as a direct-write tool to define channels with a defined topography and

adsorption contrast [183,184]. A simple wet micro contact printing technique has also been employed to generate 100 nm high non-adsorbing walls on top of motility-supporting polymer layers [185]. The use of e-beam to write nanopatterns has been made possible after testing various resist polymers for myosin activity [186,187]. Motility-resisting polymer has been coated on the top of motility supporting polymer so that patterns can be written on the top layer all the way down to the bottom layer [188]. In the next step, the undercuts developed for the kinesin–microtubule system [160] have also been included in the design [161]. Generation of unidirectional motion in the actomyosin system has been achieved by allowing filaments to enter narrow tracks through entry zones designed at only the end of the tracks [152]. Filaments enter the tracks in just one direction and cannot take U-turns because the tracks are too narrow.

5.4. Guiding using flow fields

Filament alignment using flow fields has been employed even before the concept of molecular shuttles was introduced [189,190]. Shear flow exerts drag forces on the leading tip of the gliding filament. The random tip fluctuations develop a bias towards finding a motor in the direction of the shear flow which ultimately leads to polar alignment of the entire filament in that direction [154]. However, if the pressure-driven shear flow is halted, the direction of filament movement becomes randomized again. Oriented filament arrays which support directed transport in the bead geometry are created by immobilizing the filaments immediately after alignment.

Flow-oriented microtubule arrays have served as tracks to transport micrometer sized kinesin-coated cargoes on flat surfaces [140] and in microchannels [142]. Both studies were followed by experiments with additional control over cargo movement via the use of optical tweezers [143] and varying ATP concentration [141]. Polar orientation of microtubules has also been demonstrated in a dynein-based assay [146,191] and used for unidirectional motion of both kinesin-coated and dynein-coated beads [146]. The rate of microtubule alignment at different motor densities and shear flow strengths has been investigated in [192], providing a detailed understanding of the physical mechanism underlying guiding by flow fields.

5.5. Guiding using electrical fields

Electric fields exert electrophoretic forces on the negatively charged actin filaments and microtubules, which bend the cantilevered tip of the gliding filament towards the cathode and over time, reorient the entire structure. Additional forces are exerted by the electroosmotic flow of counter ions in the opposite direction. However, the electrodes used to generate the electric fields have to be placed far apart from the filaments to alleviate the effects of heating and the generation of oxygen, which interferes with fluorescence imaging [193].

Initial fundamental studies detailing the effect of electrophoretic forces on motor-propelled actin filaments [194] and microtubules [195] have characterized the electrophoretic mobility and charge density of these filaments. Active control over the motion of individual microtubules has been achieved with electric fields [165]. In this study, populations of two differently labeled microtubules approaching a Y junction have been steered into two different reservoirs. A color-sensitive camera has been used to identify each microtubule approaching each junction and to trigger the application of the electric field in the polarity required for accurate sorting. Detailed statistical analysis of microtubule guiding by direct current (DC) fields have proved that the microtubule tip is deflected towards the anode while translocating until it is engaged by another kinesin. Hence, kinesin surface density and microtubule translocation speed along with electric field strength affect the rate of redirection of microtubules [196]. In a follow-up study, redirection behavior has been used to measure the charge density and flexural rigidity of microtubules [197].

In the presence of alternating electric (AC) fields, dielectrophoretic forces on moving filaments align them towards the highest field gradient. Although AC-generated force fields are of short range compared to static DC fields, they have been reported to be more effective than electrophoretic forces for guiding microtubules [180]. Dielectrophoretic guiding of myosin-propelled actin has also been demonstrated and analyzed [88].

5.6. Guiding using magnetic fields

Guiding using magnetic fields is made possible [198] by functionalizing filaments with ferritic particles. Microtubules functionalized with ferritic particles have been aligned [199,200] and guided [201] by externally applied weak magnetic fields. Actin filaments functionalized with superparamagnetic microspheres have been used to study the effect of externally applied loads on the motility of the actomyosin system [202].

5.7. Summary

The random motion of shuttles on the surface needs to be steered along specified paths to achieve directed transport. While initial strategies to generate unidirectional motion of shuttles [156] have been utilized to generate oriented and interconnected network of filaments for bead assays [122], strategies to actively control the shuttle motion by external means have also been demonstrated [165].

The field of guiding shuttles has now reached a matured state. The trajectory persistence length of gliding filaments has been determined experimentally [46–48,149,203,204] and the mechanistic details behind dispersion in shuttle motion have been understood [47,149]. These developments have made it possible to simulate the motion of shuttles within the structures [47,159]. Using simulations, it was discovered that the average distance traveled within a channel between two successive U-turns scales with $\exp(-0.6L_p/w)$, where L_p is the persistence length of the filament and w is the track width (Fig. 7a). The dependence of guiding efficiencies of simple motifs on the filament properties such as persistence length and motor properties such as speed was also established. This *in silico* approach

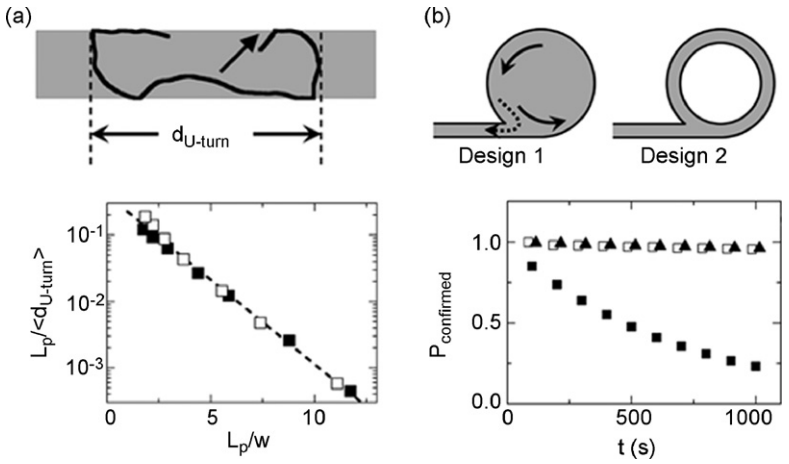

Fig. 7. (a) Simulations allow the evaluation of a filament trajectory (persistence length, L_p) in a channel (width, w) [47]. The distance between two successive U-turns, $d_{U\text{-}turn}$ scales with $\exp(-0.6L_p/w)$. Plots of actin filaments (solid squares) and microtubules (open squares) fall onto the same line: $L_p/\langle d_{U\text{-}turn}\rangle = 0.4\exp(-0.6L_p/w)$. (b) Simulations also allow the evaluation of guiding efficiencies of concentrator designs [47]. Design 1: the radius of the circle is $L_p/5$, and the width of the inlet channel is $L_p/20$. Design 2: the outer radius of the ring is $L_p/5$, and the width of the channel is 250 nm. Design 1 works well for gliding microtubules (open squares) but poorly for gliding actin filaments (solid triangles). By utilizing a ring concentrator (design 2), actin filament confinement is 40-fold improved (solid squares). Figure adapted with permission from [47]. Copyright 2008 American Chemical Society.

together with the wealth of information generated by the experimental studies enables the rational design of devices powered by biomolecular shuttles.

6. Loading and unloading of cargo

6.1. Loading and unloading approaches

In nature, kinesin-1 motors serve as motile cargo transporters moving along the stationary microtubules. Their long (~60 nm) and flexible tails are well-adapted to grasping cargo [128]. Specialized scaffolding proteins create a connection between the tail and the specific cargo [205]. Molecular shuttles, which often utilize the gliding geometry discussed in Section 4.2, require different, engineered approaches to connect with and disconnect from various types of cargo. Ideally, the cargo attachment is strong, durable, specific, reversible, adaptable to different types of cargo, and does not interfere with gliding motion of filaments [131].

The cargo-binding strategies and cargo properties have to take the characteristics of the motor/filament system into account. For example, due to their helical structure actin filaments rotate once every micrometer while being propelled by surface-adhered myosin [206,207]. If bound cargo follows the filament rotation, it might interfere with the actin–myosin interactions. In contrast, microtubules with 13 protofilaments, which can be obtained by suitable polymerization conditions [208], have their protofilament aligned parallel rather than helical to the microtubule axis. Nitzsche et al. have shown that these microtubules do not rotate while being propelled by kinesin, and, surprisingly, that attachment of large microspheres interrupts rotation of microtubules with different protofilament numbers [209].

Cargo loading onto molecular shuttles was first achieved by attaching streptavidin-coated polystyrene microspheres to kinesin-propelled microtubules [131]. It was discovered early that conjugating biotinylated microtubules with cargoes such as avidin [199], streptavidin-coated quantum dots [210] and ferritic particles [200] before introduction into the flow cell precludes subsequent binding of these filaments to the motors on the surface. To circumvent this problem, filaments can be biotinylated in segments [201,210] to define cargo binding regions and motor binding regions (Fig. 8a and b). Alternatively, cargo can be connected to filaments already bound to the surface, although, this also interferes with motor–filament interactions [211].

The connection of cargo to filaments attached to the surface-adhered motors allows for precise control over cargo dosage and localized cargo binding. The filaments are held to the surface by the motors, hence cargo can be introduced and removed by buffer exchanges. This technique has enabled the evaluation of the attachment kinetics of streptavidin to biotinylated microtubules [215] and of the effect of size and concentration of a variety of cargoes [212] on motility. A precise knowledge of dosage-coverage characteristics is critical in applications such as active self-assembly of filaments [216–219]. Localized cargo binding has been achieved by defining surface regions with high cargo densities (yellow region in Fig. 8c) [213,220]. Cargo has been specifically immobilized with tethers utilizing reversible chemistries. Kinesin-driven functionalized microtubules have then picked up cargo from these 'loading stations' and transported it to cargo-free areas. This design spatially separates cargo pick-up and its subsequent utilization.

Cargo can be attached to filaments using covalent as well as non-covalent chemistries. However, non-covalent interactions, such as antibody/antigen bonds are preferred due to their selectivity and reversibility. In particular the strong non-covalent bond between biotin and streptavidin is readily integrated into molecular shuttle systems due to the commercial availability of biotinylated tubulin and actin (Cytoskeleton Inc.).

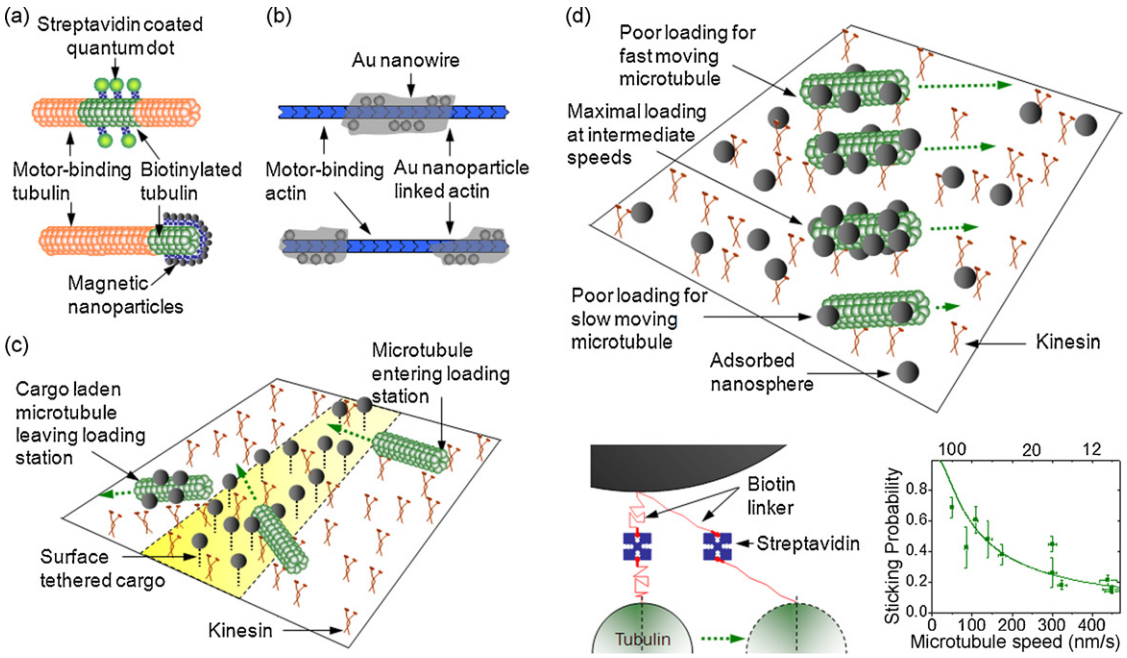

Fig. 8. Considerations for cargo loading onto kinesin driven microtubules. Cargo binding to (a) microtubules [201,210,212] and (b) actin [63] prior to motor binding precludes filaments from binding to motors. Hence cargo should be bound to filaments in segments with defined regions for cargo binding and motor binding. (c) Spatial control over cargo binding can be achieved by engineering 'loading stations' [213] on a surface. These stations have cargoes tethered to the surface by reversible chemistries. Figure adapted from Brunner et al. [213]. Copyright The Royal Society of Chemistry. Reproduced with permission. (d) Biotin–streptavidin behaves as a molecular adhesive over the timescales of binding of surface adsorbed cargo to moving microtubules. Hence, microtubule speed has to be optimized to maximize cargo binding to the filaments [214]. Figure adapted with permission from [214]. Copyright 2009 American Chemical Society.

Biotinylated microtubules, sometimes coated with streptavidin, have carried a wide variety of streptavidin-functionalized or biotinylated cargoes, including quantum dots [210], micro- and nanospheres [131,212] (Fig. 9a), ferritic particles, [199–201], DNA [221–224] and carbon nanotubes [225]. Biotinylated microtubules have been shown to transport, stretch [221], and manipulate [222,223] biotinylated DNA molecules via streptavidin cross-links. DNA-loaded microtubules have been used to test the sensitivity and selectivity of the capture of complementary fluorescent DNA strands (Fig. 9b) [224]. In a substantially improved design [226], microtubules carried single-stranded DNA with a fluorescence tag in the quenched state (a so-called 'molecular beacon'). Capture of complementary strand from solution opened the beacon, thus enhancing its fluorescence.

A surprising dependence of cargo loading on the shuttle speed has been observed for biotin/streptavidin linkages [214]. Surface-adsorbed biotinylated nanospheres have been picked-up by streptavidin-functionalized moving microtubules. Cargo attachment is maximal at a speed of ~200 nm/s, which is significantly below the top speed of the shuttle. The optimum is a consequence of the complex binding energy landscape of the biotin–streptavidin linkages, which gain their ultimate strength on a time scale of milliseconds. This insight relies on a detailed analysis of the mechanics and chemistry of the binding process, where the flexible biotin linkers on the microtubule and

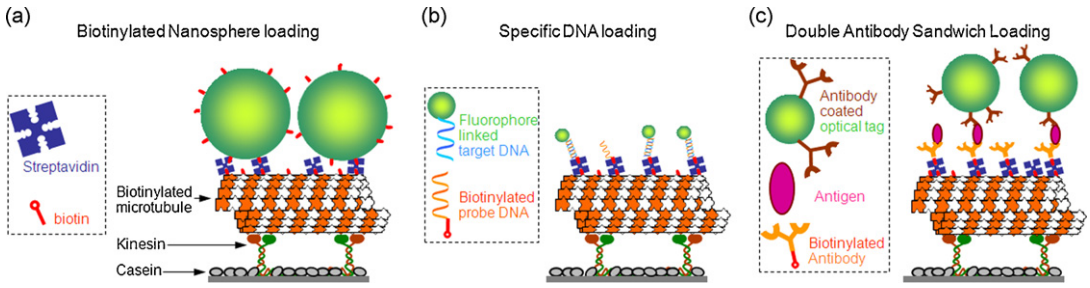

Fig. 9. Examples of loading experiments utilizing the biotin–streptavidin chemistry. (a) Biotinylated cargo, such as biotinylated nanospheres can be attached to streptavidin-coated biotinylated microtubules [214]. (b) Specific capture of fluorophore-linked target DNA has been shown by microtubules functionalized with appropriate probe DNA. The biotinylated probe strands where attached to biotinylated microtubules using streptavidin as a cross-linker [224]. (c) A double-antibody-sandwich assay was realized by linking a biotinylated antibody to a biotinylated microtubule with streptavidin, selectively capturing analytes from solution, and detecting the captured analytes via binding of antibody-functionalized optical tags [215,227–230].

the nanosphere can stretch from their most probable end-to-end distance to their maximum contour length (shown in Fig. 8d) and where attachment is governed by force-dependent reaction rates.

A major advance in loading cargo onto shuttles has been the attachment of cargo without prior biotin/streptavidin functionalization. Analytes, such as myoglobin proteins [215] and virus particles [227], were directly captured by antibodies attached to the shuttle. In combination with the pick-up of a second antibody carrying an optical tag, a double-antibody-sandwich has been constructed on gliding microtubules (Fig. 9c). In a related development, capture and transport of engineered cargo such as cowpea mosaic virus (CPMV) particles [228] has been demonstrated using both avidin–biotin and antibody–antigen interactions. It was envisioned that the quantum dot-functionalized virus could simultaneously serve as a bright fluorescent tag and as a portable scaffold for biomolecules. In a follow-up study [229], these virus particles have carried fluorescent groups as well as antibodies to a toxin, staphylococcal enterotoxin B (SEB). A double-antibody-sandwich assay was used to successfully load these CPMV particles onto gliding microtubules. This technology has recently been expanded to multi-analyte assays [230], opening avenues for the design of multiplex biosensors.

Other creative cargo-loading schemes have provided shuttles' systems with cargo unloading capability [220,231,232] and with an *in situ* supply of fuel [233]. Malachite green loaded onto microtubules has been shown to capture and release malachite green aptamers [231]. The aptamer release is triggered by adding excess malachite green to the motility buffer. In another report, cyclodextrin has been loaded onto microtubules [234]. Cyclodextrin molecules can reversibly bind certain guest molecules in their cavity. The capture of 1,8-ANS molecules by cyclodextrin-loaded microtubules has been demonstrated, although unloading is not yet demonstrated. For incorporating an *in situ* supply of fuel, microspheres coated with an ATP-generating enzyme have been loaded onto microtubules through the biotin–streptavidin chemistry [233]. Unfortunately, the limited amount of enzyme present restricts the gliding velocities to about 1% of the maximum speed.

Cargo loading onto gliding actin filaments has been shown for a limited number of systems. Polystyrene microspheres have been coated with gelsolin, a protein selectively binding to the barbed end of actin [235]. Actin filaments loaded these microspheres specifically at the trailing end, and glided on myosin-coated surfaces without any significant reduction in velocity [235,236]. Loading biotinylated actin filaments with streptavidin-coated quantum dots also preserved the ability to glide [237]. Similar to preparation of segmented microtubules with defined regions for cargo binding and motor binding [210], segmented actin filaments [63] have been prepared from native actin monomers and actin monomers functionalized with gold nanoparticles. Gold nanoparticles have been grown into wires within defined segments of the actin filaments by catalytic enlargement of the nanoparticles (Fig. 8b). About 40% of these segmented gold nanowire-actin filament polymers are capable of being propelled by surface immobilized myosin [63].

6.2. Summary

Our ability to load cargo onto molecular shuttles has rapidly advanced. A wide variety of cargo has been successfully loaded, and the developed techniques have been integrated in device applications. In particular, the loading of DNA molecules [221] and assembly of double-antibody-sandwich assays onto moving shuttles [215,227] have inspired studies of single molecule manipulation [222] and biosensors [132,238], respectively. In addition, recent studies have identified the effects of cargo loading on the motility of shuttles [211,212] and the dependence of cargo loading on shuttle speeds [214].

Controlled unloading of cargo would be beneficial for various molecular shuttle designs. Shuttles would be able to transfer cargoes between different stations [213,220], and could also be used multiple times. Initial studies into controlled breaking of linkages [239] and interactions between cargo-loaded microtubules [240] provide important insights for designing such arrangements.

7. Controlling motor activity

7.1. Activation approaches

Biomolecular motors are enzymes of the ATPase family and can be described by the Michaelis–Menten model for enzyme kinetics [241]. Production of motion is typically dependent on ATP consumption, hence controlling ATP concentration is a direct route to controlling shuttle velocity. In addition, the dependence of motor activity on a variety of other factors such as divalent ion concentrations, pH, temperature and motor density has been investigated for kinesin [242–244] and myosin [245–248].

Thus, motor activity can be reversibly controlled over time by changing the concentration of ATP [249–251], by reversibly inhibiting motors with local anesthetics [252,253], or by engineering kinesin mutants with activity depending switch-like on the presence of Ca^{2+} [254] or Zn^{2+} [255]. With advanced microfluidic perfusion systems, these concentration changes can be achieved under computer control within seconds. For example, kinesin-propelled microtubules can be stopped within 1 s and restarted within 10 s [256]. However, the use of solution exchanges to regulate motor activity is inconsistent with the application of molecular shuttles as an alternative to fluid flow.

An alternative approach to changing the concentration of molecular activators or inhibitors is the use of caged compounds. For example, 1-(4,5-dimethoxy-2-nitrophenyl)ethyl-caged ATP (DMNPE-caged ATP) converts from an inactive to an active state upon exposure to UV light, and the released ATP can be subsequently sequestered by an ATP-consuming enzyme, such as hexokinase [131]. This creates a temporary increase in ATP concentration which translates into shuttle movement over micrometer distances. In a follow up study [258], the optical and biochemical properties of DMNPE-caged ATP

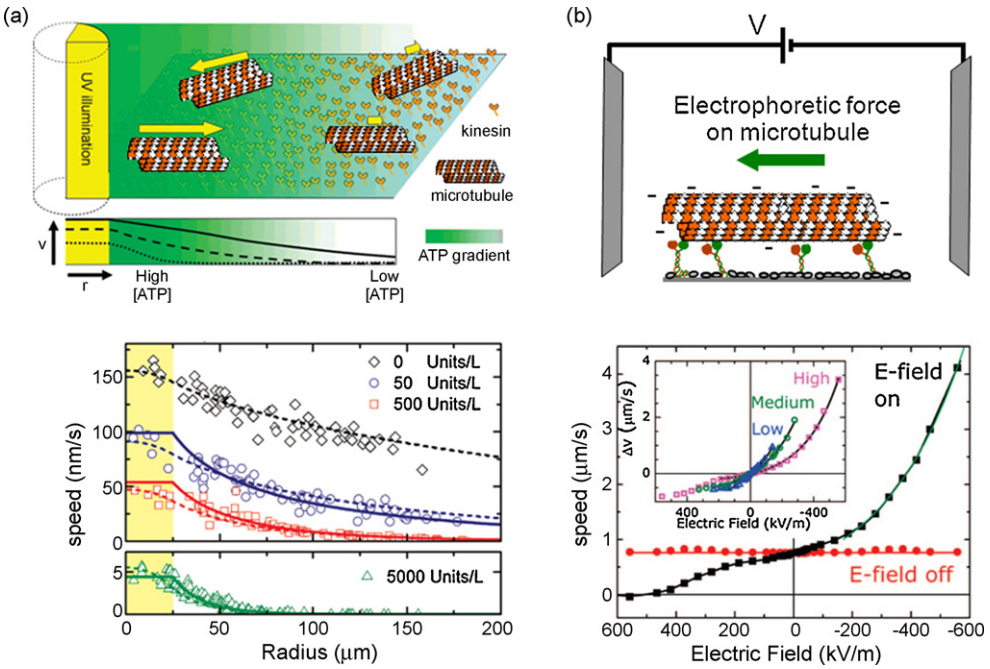

Fig. 10. (a) Light activation and control of molecular shuttles [67]. A cylindrical cone of UV light locally photolyzes caged-ATP to produce ATP. As the ATP diffuses outward, it is hydrolyzed by kinesin and consumed by hexokinase. Addition of hexokinase increases the gradient of the ATP concentration profile at the expense of the maximum shuttle speed. Figure reproduced with permission from [67]. Copyright 2008 American Chemical Society. (b) Manipulation of microtubule speeds with electric field [257]. Negatively charged microtubules move faster in the presence of assisting fields by a factor of 5 and can be completely stalled in the presence of opposing fields. Figure reproduced with permission from [257]. Copyright 2008 American Chemical Society.

have been characterized in detail. It has also been demonstrated that DMNPE-caged ATP can be stored in sufficient amounts in a typical device and that the activation can be triggered with a UV lamp or even sunlight. To gain additional spatial and temporal control over motor activity, UV exposure can be carried out in short pulses and through small pinholes (Fig. 10a) [67]. Photolysis of caged inhibitors to decrease motor speed has also been achieved [259]. Based on the knowledge that the kinesin tail domain suppresses the ATPase activity of the motor domain, caged peptides derived from the kinesin tail domain have been engineered. Upon uncaging by photolysis, these peptides interfere with kinesin motility and reduce speeds to 20% within 20–30 s of exposure.

Changes in temperature cause exponential variations in the enzymatic activity of motors [243,244]. Temperature-pulse microscopy, which utilizes laser light for heating, enables highly localized and rapid temperature changes. The technique has been utilized to control both myosin [260] and kinesin [261] activity. Rapid temperature changes have also been realized using an all-electrical system [262]. Thin metallic film heaters and thermometers have been fabricated onto a single glass cover slip and biased by a DC voltage. Electrically controlled thermal activation of myosin motors has been studied in the temperature range from 10 °C to 50 °C [262]. The speed of microtubules gliding over a kinesin-coated surface has also been directly controlled by the application of an electric field. Negatively charged microtubules experience an electrophoretic attraction towards the cathode (Fig. 10b). Although electric fields have been primarily used to guide the direction of filament motion, it was shown that the microtubule gliding speeds can increase five-fold by application of assisting fields or decrease to zero for opposing fields [257]. A simple grab-and-release model has been used to explain the velocity change with applied electric fields.

Smart surfaces coated with stimuli-responsive polymers [263] enable elegant alternatives to motor control. Chains of the thermoresponsive polymer poly(N isopropyl acrylamide) (PNIPAM) with embedded functional kinesin have been grafted onto a silicon substrate [264]. Conformational changes have been induced in the PNIPAM chains via external temperature control. Above the lower critical solution temperature (32 °C) polymer chains are compacted and microtubules can land and glide on the kinesin surface. At lower temperatures, the chains extend to more than 20 nm above the surface and the microtubules are released from the surface. This effect can be understood to be a result of the geometry of the gliding filament [128]. In a follow-up study [8], PNIPAM polymer chains with different transition temperatures have been immobilized on the surface. This allows for active control over the size of surface regions in which PNIPAM is swollen or collapsed. A fundamentally different design employs an electrically switchable surface [265]. When the polymer (poly(CH_2OH-EDOT)) is electrochemically switched from its semiconducting state to its conducting state, the speed of microtubule gliding on adsorbed kinesin decreases reversibly by 35%. This reversible interaction of enzyme activity with surface properties is a surprising finding of possibly far-reaching impact.

While regulating motor activity is one approach, recent reports have aimed to manipulate filament density and velocity without targeting the motors. Reversible docking of negatively charged microtubules has been demonstrated on gold microfabricated surfaces by electrostatic fields [266].

7.2. Summary

Flow-based exchange of buffers can modulate the activity of wild type or mutant kinesins by effecting changes in the buffer composition. However, motor activities can be more elegantly controlled by external stimuli such as changes in temperature, light-controlled release of caged ATP, and application of electrical fields.

The spatial and temporal resolution of the control mechanism is often limited by diffusion of either control molecules or heat. In order to control the activity of individual shuttles, the concentration profile of the activator or inhibitor molecules needs to be sharpened. To prevent diffusion of control molecules beyond the desired zone of activation, a sequestration system can be employed. However, the increased spatial control comes at the expense of a reduced efficiency in the utilization of the control molecules [67].

Activation methods based on localized heating are in addition limited by the small temperature span within which motor proteins retain their functionality. While the electric modulation of surface properties [265] to control motor activity does not yet deliver the desired reduction of the gliding speed to zero, it likely does not suffer from similar constraints with respect to spatial and temporal control.

8. Applications

In this section we highlight some of the general application concepts that have emerged from the integration of molecular motors and synthetic components. There have been intriguing reports proposing motor-based nanotechnologies such as micropumps [267] and biocomputation devices [268]. Here we focus on experimental demonstrations which incorporate the technical approaches outlined in the preceding sections.

8.1. Manipulation of single molecules

Recent studies [62,67] have argued that shuttles are best utilized in a 'swarm' context rather than as tightly controlled individual nanotransporters. Nevertheless, the reproducible and well-characterized nanoscale motion generated by motors and the ability to attach cargo via bioconjugation techniques onto filaments has inspired several single molecule manipulation studies.

Interactions between cargo-carrying shuttles are routinely studied using fluorescence techniques [240]. In an early study [269], a collision between a surface-immobilized biotinylated microtubule and a kinesin-propelled biotinylated microtubule carrying a streptavidin-coated microsphere has been analyzed (Fig. 11a). The clamped microtubule serves as a molecular cantilever and the moving microtubule applies a bending force on it once the microsphere attaches to the cantilever. In the event of a transfer of the bead, the bending force can be estimated using the known stiffness of a microtubule. This arrangement can serve as a versatile forcemeter for measuring rupture forces of single receptor/ligand pairs in the pN range.

Significant progress has also been achieved for DNA transport and manipulation. Kinesin-propelled biotinylated microtubules havee been used to transport and stretch individual λ-phage DNA molecules [221]. DNA molecules, biotinylated at their ends, are attached to the microtubule via a streptavidin linkage. DNA stretching was achieved when a moving microtubule picked up the end of another DNA molecule already attached to the substrate at its other end (via streptavidin or pH-dependent binding to the glass). This design has been further improved

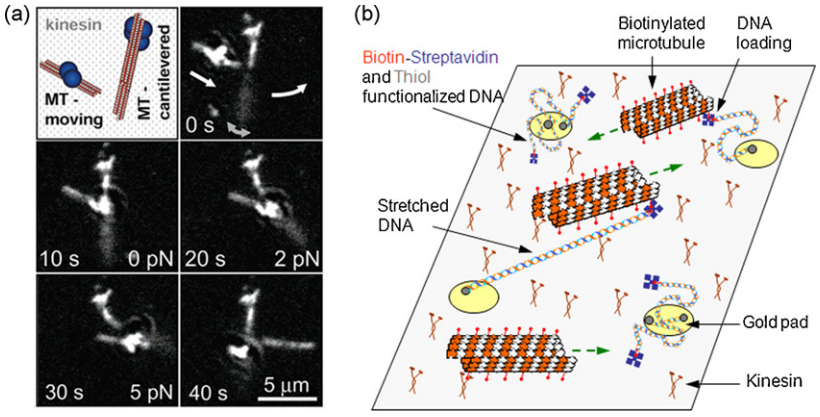

Fig. 11. Manipulation of single molecules. (a) A cantilevered microtubule is loaded by a kinesin propelled microtubule due to biotin–streptavidin chemistry. As the stiffness of the microtubule is well characterized, the bending of the microtubule at the point where the linkage breaks can be used to estimate the force required to break the linkage [269]. Figure reproduced with permission from [269]. Copyright 2002 American Chemical Society. (b) DNA molecules with thiol groups at one end were stuck to the surface within defined gold pads. The other end carried biotin–streptavidin, which was used to load that end onto the gliding biotinylated microtubules. DNA loading onto moving microtubules and subsequent transport results in unwinding and stretching of the DNA strands [221–223]. Figure adapted from Dinu et al. [222]. Copyright Wiley-VCH Verlag GmbH & Co. KGaA. Reproduced with permission.

by attaching the stationary end of the DNA double strand to the surface by thiol/gold linkages (Fig. 11b) [222]. This allows for greater spatial control over the parallel manipulation of DNA molecules between the microfabricated gold pads and motile microtubules. In a related study [223], DNA molecules have been tethered to the surface by antibody–antigen interactions and the other end has been stretched by motile microtubules. The stretched DNA molecule is then immobilized between the bottom coverslip and a top polyacrylamide gel and cleaved by an enzyme supplied through the gel.

8.2. Investigation of surface properties

Biomolecular shuttles interface biological and synthetic components. While considerable efforts have been expended in maintaining the function of the incorporated proteins in their new environment [29], some studies exploit the protein functionality to characterize the environment around them.

In the first report which probed surface topographical features using molecular shuttles [270], fluorescent microtubules were propelled randomly by kinesin on a topographically structured surface (Fig. 12a). Microtubules visited the elevated portions of the surface less often which showed up as dark spots in an image created by overlaying hundreds of fluorescence microscopy images acquired successively from the same surface region.

This concept has been expanded to include local height information with the use of fluorescence-interference contrast (FLIC) wide-field microscopy. FLIC microscopy encodes height information with nanometer resolution for a fluorophore situated above a reflecting surface by exploiting interference effects for excitation and emission light. To demonstrate imaging in three dimensions, surface topographies have been patterned into a silicon oxide layer [127] (Fig. 12b). Kinesin-driven microtubules cross shallow and deep pits and change their distance from the underlying reflective silicon substrate. At high motor densities, the trajectories of the flexible microtubules reproduce the topography of the surface, which can be inferred from the fluorescence intensities. This parallel process relying on autonomous, self-propelled nanorobots is a conceptual alternative to the deterministically controlled macroscopic cantilever probes of scanning force microscopes.

The strong interaction between kinesin and microtubules has also been explored as a technique for quantifying the surface coverage of functional kinesin at extremely low densities (Fig. 12c). Measuring the rate of microtubule attachment from solution to surface-adhered kinesin enables the determination of motor densities down to a few motors per μm^2 [104,108]. Although microtubule landing rates have been used to compare functional kinesin densities on different surfaces for guiding purposes [178,179], an absolute determination of kinesin densities has not been attempted. In a recent report [123], functional kinesin densities in the range of 0.004–1 ng cm^{-2} have been measured to evaluate the performance of several state-of-the-art non-fouling surface chemistries. This method offers a substantial improvement over the detection limit of established characterization techniques, such as surface plasmon resonance (which is about a ng per cm^2).

8.3. Self-assembly

Molecular self-assembly is the spontaneous association of molecular-scale components into a hierarchical organization by attractive forces [271]. Self-assembled structures can be prepared in large numbers in parallel from bottom up and are envisioned to replace the prod-

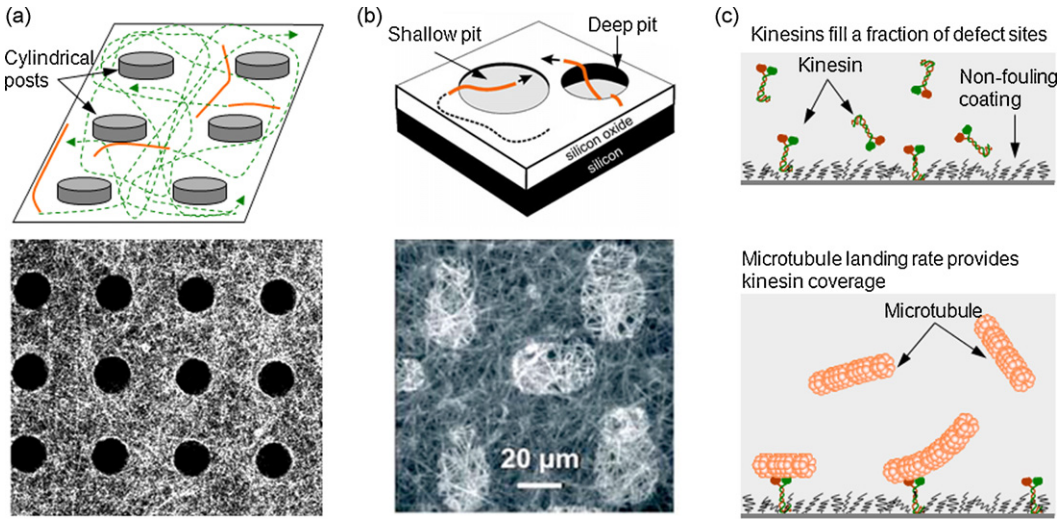

Fig. 12. Investigation of surface properties using molecular shuttles. (a) Information about surface topography can be revealed in a time-integrated image of microtubules moving randomly on the surface [270]. Figure reproduced with permission from [270]. Copyright 2002 American Chemical Society. (b) The height of the topographical features can also be quantitatively deduced by the utilization of fluorescence-interference contrast (FLIC) wide-field microscopy [127]. Figure reproduced from Kerssemakers et al. [127]. Copyright Wiley-VCH Verlag GmbH & Co. KGaA. Reproduced with permission. (c) Quantification of functional kinesin density on a surface [123]. In the first step, the test surface is exposed to a known dosage of kinesin. Kinesin is then exchanged by a microtubule solution of known concentration. At low kinesin coverages, the landing rate of microtubules is directly proportional to the functional kinesin density on the surface.

ucts from serial top down nanofabrication techniques such as scanning tunneling microscopy and e-beam lithography. Self-assembly, in most cases, does also not require high vacuum, clean room environment or cryogenic temperatures.

Traditionally, self-assembly at the molecular scale relies on diffusion to bring the building blocks in contact and on thermal activation to break unintended contacts. The complex attractive and repulsive interactions required for structures composed of different building blocks need to be already encoded into the basic units. For example, the highly specific interactions between nucleotides of several short DNA strands have been used to generate well defined 'DNA origami' geometries [272]. In a 'one-pot' technique, strands are mixed together at elevated temperatures and left to anneal for a few hours to self-assemble into the desired structures.

It has been argued however, that distinct advantages can be conferred to the assembly process if the building blocks are actively transported by molecular shuttles [217]. Besides accelerating the process for larger structures, it facilitates the utilization of stronger bonds. Instead of relying on thermal activation to dissociate mismatched parts,

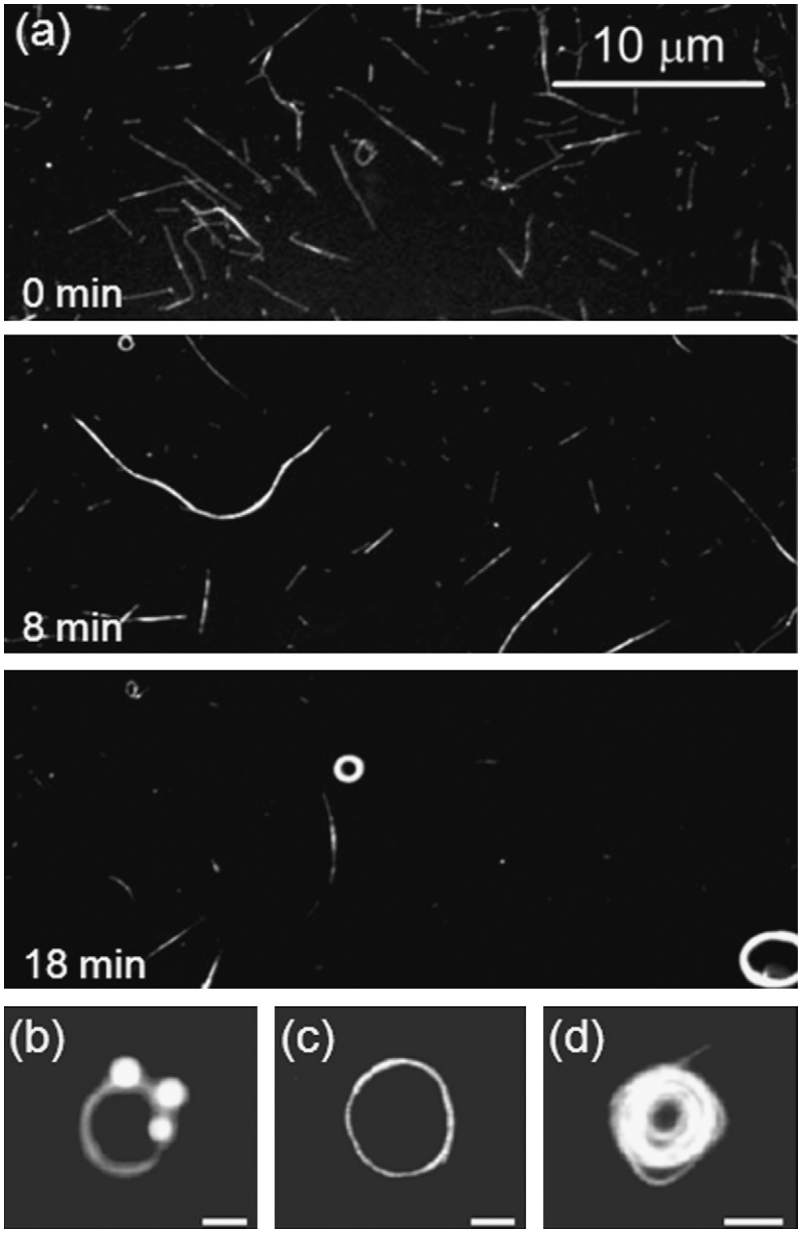

Fig. 13. Non-equilibrium self-assembled structures obtained from 'sticky' microtubules propelled by kinesin [212,216,218,219]. Biotinylated microtubules partially coated with (a) streptavidin or (b) streptavidin coated microspheres or (c and d) streptavidin quantum dots result in nanowires and nanospools. Scale bars in (b), (c) and (d) represent 2 μm. (a) Reproduced with permission from [216]. Copyright 2005 American Chemical Society; (b), (c) and (d) reproduced with permission from [212]. Copyright American Scientific Publishers.

force generated by motors can be used to rectify errors in assembly. Most importantly, it permits the assembly of strained, non-equilibrium structures.

Self-assembled strained structures can be produced by kinesin-driven biotinylated microtubules by partially covering the microtubule surface with streptavidin [216,219] or streptavidin-coated quantum dots [212]. The gliding microtubules first assemble into 'nanowires', which in turn form 'nanospools' (Fig. 13). Motors play a crucial role in the assembly of both the structures. All the microtubules in the nanowire are aligned in a unipolar fashion. The motor force insures that the initial contacts between wrongly aligned microtubules are broken. Motors also provide the bending force for stiff microtubules to assemble into nanospools. These final strained structures are stable, because multiple biotin–streptavidin bonds keep them in place. If however, excess biotin is added after the structures are formed, motor action leads to disassembly [218], revealing the reversibility of the process. Dynamic assembly of these structures can thus be understood as an interplay between thermodynamic and energy-consuming processes [218].

8.4. Biosensing

The active transport of proteins and viruses enabled by molecular shuttles is a valuable tool in the context of lab-on-a-chip devices, since it can be exploited to concentrate analytes [238] or to replace mass transport by pressure-driven fluid flow or electroosmotic flow [149].

The capture and concentration of analytes by molecular shuttles has been experimentally demonstrated by aggregating streptavidin (serving as analyte) with biotinylated microtubules moving on a kinesin-coated surface structured into a large capture area and a small collection area [238]. If carefully designed, such a capture and collection process can accelerate analyte arrival at the sensor site up by orders of magnitude [150].

Replacing other mass transport mechanisms provides a particular benefit for "smart dust" devices [273] which during their autonomous operation can ill afford external electrical power or external pumps. Based on the molecular shuttle technology described in the preceding sections, a miniaturized integrated analytical device which detects the presence of antigen in a complex solution has now been reported [132].

In a biosensor, analytes are often detected by specific capture with receptor molecules and subsequent tagging with optical tags. A common strategy, especially for protein and virus analytes, is to employ a double-antibody-sandwich assay. In such assays, excess sample solution has to be removed after the capture process and unbound optical tags have to be removed before the detection process. These solution exchanges are usually driven by external pumps or manual pipetting. Molecular shuttles provide the possibility of replacing the capture–wash–tag–wash–detect sequence in these assays with a capture–transport–tag–transport–detect sequence (outlined in Fig. 14).

Several key developments have enabled such a design. Successful assembly and transport of double-antibody-sandwich assays by molecular shuttles [215,227,229] has been demonstrated for a variety of antigen types and now, for different analytes in the same assay [230]. Spatial control over pick up and delivery of cargoes has been achieved by designing loading stations [213]. This is critical because in the shuttle-based biosensor design, functionalized shut-

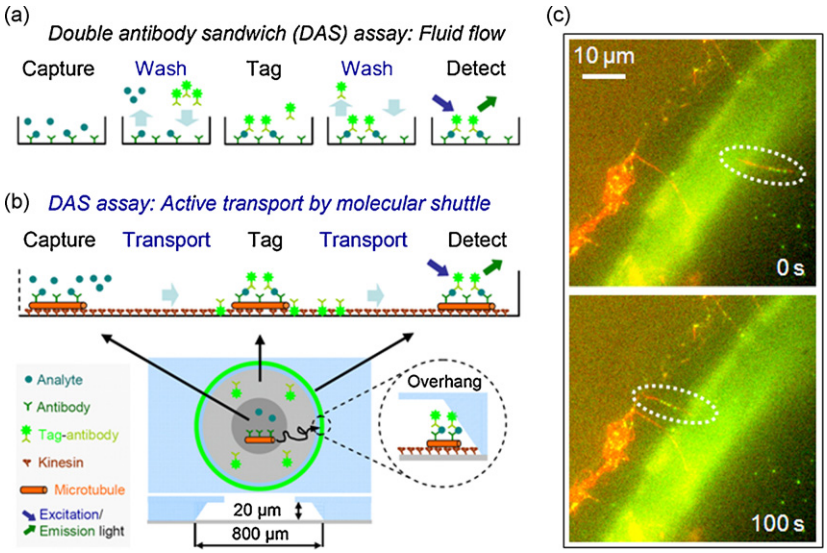

Fig. 14. (a) A device utilizing active transport can substitute the washing steps intrinsic to a double-antibody-sandwich assay with transport mediated by biomolecular motors. (b) Design of a 'smart dust' biosensor which employs biomolecular mediated transport in the formation of a double-antibody-sandwich to capture and tag antigens and moving it to a detection area [132]. (c) Biotinylated and rhodamine-labeled microtubules (red) loaded with biotinylated nanospheres (green) travel from the tagging zone into the detection zone and get immobilized there. The accumulation of nanosphere-loaded microtubules in the detection zone (under the overhang) is the signal indicative of the presence of streptavidin. A band of immobilized microtubules with optical tags attached to them can be seen in the detection zone. Figure reprinted by permission from Macmillan Publishers Ltd.: Nature Nanotechnology [132], Copyright 2009. (For interpretation of the references to color in this figure legend, the reader is referred to the web version of the article.)

tles would capture antigens and then move into a tagging zone to pick up the optical tags. Shuttles loaded with optical tags can also be collected into a centralized small location to enhance the signal from the tags. This has been demonstrated [238] by concentrating biotinylated microtubules which captured labeled streptavidin at the center of a spiral pattern. Challenges regarding controlled activation of motors [67], maximal loading of shuttles [214], and long term storage and operation of the overall hybrid device [274,275] have also been investigated in detail.

Successful incorporation of these building blocks has led to the development of a biomolecular motor-powered smart dust biosensor [132]. In this biosensor, gluthathione-S-transferase (GST) serves as the analyte. Biotinylated GST antibodies are linked to biotinylated microtubules via streptavidin, and quantum dots conjugated to the second GST antibody serve as optical tags. A microdevice with the shape of a flat well has been fabricated (Fig. 14b). Optical tags remain suspended in the solution and hence a separation of zones for analyte pick-up and tagging has been abolished. GST and optical tags have been captured onto functionalized microtubules, which move randomly on the flat surface of the device and then get immobilized at the sidewall. Furthermore, the sidewall exhibits extended overhangs, which prevents optical tags from reaching the sidewall by diffusion. The surface under the overhangs thus serves as an effective detection zone. GST at nanomolar concentration has been successfully detected within a few hours. Although there is significant scope for optimization of device parameters towards improving the sensitivity of the device, it represents the first prototype which tags, transports, deposits and detects unlabeled analytes.

9. Conclusions and outlook

Nanoscale engineering with biomolecular motors has blossomed in the past decade, but it still remains a scientific frontier. While some technologies proceed in a series of incremental steps, where each new device generation resembles the previous generation in its design and function, the field of molecular motor engineering represents a fresh approach to the challenge of purposefully converting chemical energy into mechanical work. As a result, the field has to develop an ecosystem of application ideas, which give direction to its future development.

Two distinct technology trends create a “pull” for the field. Firstly, the number of motors utilized in our lives is constantly increasing while their size is steadily decreasing. For example, a Ford T model of 1909 had exactly one motor while a modern car incorporates dozens of motors, including two motors operating the CD player. Creating the technology to produce minute amounts of mechanical work is almost certainly of significant future utility. The above-described ‘Smart Dust’ biosensor pushes this to the extreme by utilizing femtoNewtons of force to transport a small number of molecules.

Secondly, the direct and “cold” conversion of chemical energy into mechanical work is a so far unused route in technology. The currently dominant path from chemical energy over heat to mechanical work is beginning to be replaced by the pathway leading from chemical energy over electricity (via fuel cells) to mechanical work. In comparison, utilizing macroscopic arrays of molecular motors may enable efficiency gains as well as a reduction in the complexity of the system.

A third, scientific raison d’être for this work can be seen in the context of synthetic biology. Our ability to design complex biological system hinges on our understanding of the relevant mechanical engineering issues just as much as on our ability to program the genetic code. The ‘form’ of a biological system is constrained by physical laws as D’Arcy Thompson discussed [276], and these, often non-obvious, constraints will also be encountered when designing engineered *in vitro* systems. Mastering the design of hybrid systems will thus enable us to understand the choices made by evolution in more depth [277].

Nevertheless, significant challenges to real-world applications exist, first and foremost the limited stability of the biological components. Biomolecular motors and cytoskeletal filaments have to be maintained in aqueous solution of precise pH and ionic composition to prevent denaturation. Even under optimal environmental conditions, biological components are less stable than the less functional synthetic components and are regularly replaced in biological systems. Secondly, the hierarchical assembly of structures over multiple length scales, which is so beautifully exhibited by muscle tissue, has not yet been achieved. These challenges are of a fundamental nature and common to many fields within nanobiotechnology. It may take decades to resolve them or to develop synthetic components as replacements of the biological parts, just as it has taken decades to develop other technologies. However, we consider it a privilege to work on large problems.

Despite the interdisciplinary nature of this engineering frontier, polymer science concepts have proven to be critical for an understanding of the observations and conversely the employed structures illustrate polymer science concepts with particular vividness. The distance between a microtubule and the kinesin-coated surface is determined by the radius of gyration of the kinesin tail [128]. The statistical properties of the trajectory of a gliding microtubule are efficiently described by a persistence length [47]. The concept of a molecular weight distribution can be visually experienced by students examining the length distribution of microtubules polymerized from tubulin.

In summary, biomolecular motor engineering is driven by diverse goals beyond the initial vision of nanoscale transporters controlling the assembly of molecular building blocks in nanoscale factories. Convergence with efforts to design synthetic molecular motors by bottom-up [12,278] or top-down [279] assembly will further strengthen the vitality of the field.

Acknowledgement

Financial support was provided by NSF grant DMR-0645023.

References

[1] Hunt AJ, Gittes F, Howard J. The force exerted by a single kinesin molecule against a viscous load. Biophys J 1994;67:766–81.

[2] Schmiedl T, Seifert U. Efficiency of molecular motors at maximum power. EPL 2008;83, 30005/1–6.
[3] Yoshida R, Sakai T, Ito S, Yamaguchi T. Self-oscillation of polymer chains with rhythmical soluble–insoluble changes. J Am Chem Soc 2002;124:8095–8.
[4] Yoshida R, Takei K, Yamaguchi T. Self-beating motion of gels and modulation of oscillation rhythm synchronized with organic acid. Macromolecules 2003;36:1759–61.
[5] Yeghiazarian L, Mahajan S, Montemagno C, Cohen C, Wiesner U. Directed motion and cargo transport through propagation of polymer-gel volume phase transitions. Adv Mater 2005;17:1869–73.
[6] Yeghiazarian L, Arora H, Nistor V, Montemagno C, Wiesner U. Teaching hydrogels how to move like an earthworm. Soft Matter 2007;3:939–44.
[7] Ionov L, Sapra S, Synytska A, Rogach AL, Stamm M, Diez S. Fast and spatially resolved environmental probing using stimuli-responsive polymer layers and fluorescent nanocrystals. Adv Mater 2006;18:1453–7.
[8] Ionov L, Synytska A, Diez S. Temperature-induced size-control of bioactive surface patterns. Adv Funct Mater 2008;18:1501–8.
[9] Stayton PS, Shimoboji T, Long C, Chilkoti A, Chen GH, Harris JM, et al. Control of protein–ligand recognition using a stimuli-responsive polymer. Nature 1995;378:472–4.
[10] Ding ZL, Fong RB, Long CJ, Stayton PS, Hoffman AS. Size-dependent control of the binding of biotinylated proteins to streptavidin using a polymer shield. Nature 2001;411:59–62.
[11] Chen Y, Wang MS, Mao CD. An autonomous DNA nanomotor powered by a DNA enzyme. Angew Chem Int Ed 2004;43:3554–7.
[12] Bath J, Turberfield AJ. DNA nanomachines. Nat Nanotechnol 2007;2:275–84.
[13] Smith NP, Barclay CJ, Loiselle DS. The efficiency of muscle contraction. Prog Biophys Mol Biol 2005;88:1–58.
[14] Dixit R, Ross JL, Goldman YE, Holzbaur ELF. Differential regulation of dynein and kinesin motor proteins by tau. Science 2008;319:1086–9.
[15] Gordon AM, Homsher E, Regnier M. Regulation of contraction in striated muscle. Physiol Rev 2000;80:853–924.
[16] Humphrey D, Duggan C, Saha D, Smith D, Kas J. Active fluidization of polymer networks through molecular motors. Nature 2002;416:413–6.
[17] Smith D, Ziebert F, Humphrey D, Duggan C, Steinbeck M, Zimmermann W, et al. Molecular motor-induced instabilities and cross-linkers determine biopolymer organization. Biophys J 2007;93:4445–52.
[18] Bachand GD, Montemagno CD. Constructing organic/inorganic NEMS devices powered by biomolecular motors. Biomed Microdev 2000;2(3):179–84.
[19] Soong RK, Bachand GD, Neves HP, Olkhovets AG, Craighead HG, Montemagno CD. Powering an inorganic nanodevice with a biomolecular motor. Science 2000;290:1555–8.
[20] York J, Spetzler D, Xiong FS, Frasch WD. Single-molecule detection of DNA via sequence-specific links between F-1-ATPase motors and gold nanorod sensors. Lab Chip 2008;8:415–9.
[21] Hess H, Vogel V. Molecular shuttles based on motor proteins: active transport in synthetic environments. Rev Mol Biotechnol 2001;82:67–85.
[22] Hess H, Bachand GD, Vogel V. Motor proteins in synthetic materials and devices. In: Schwarz JA, Contescu C, Putyera K, editors. Encyclopedia of nanoscience and nanotechnology. New York: Marcel Dekker; 2004.
[23] Hess H, Bachand GD, Vogel V. Powering nanodevices with biomolecular motors. Chem Eur J 2004;10:2110–6.
[24] Diez S, Hellenius JH, Howard J. Biomolecular motors operating in engineered environments. In: Niemeyer CM, Mirkin CA, editors. Nanobiotechnology. Weinheim: Wiley-VCH; 2004.
[25] Hess H, Bachand GD. Biomolecular motors. Mater Today 2005;8:22–9.
[26] Mansson A, Sundberg M, Bunk R, Balaz M, Nicholls IA, Omling P, et al. Actin-based molecular motors for cargo transportation in nanotechnology—potentials and challenges. IEEE Trans Adv Packaging 2005;28:547–55.
[27] van den Heuvel MGL, Dekker C. Motor proteins at work for nanotechnology. Science 2007;317:333–6.
[28] Bakewell DJG, Nicolau DV. Protein linear molecular motor-powered nanodevices. Aust J Chem 2007;60:314–32.
[29] Fischer T, Hess H. Materials chemistry challenges in the design of hybrid bionanodevices: supporting protein function within artificial environments. J Mater Chem 2007;17:943–51.
[30] Mansson A, Balaz M, Albet-Torres N, Rosengren KJ. In vitro assays of molecular motors—impact of motor–surface interactions. Front Biosci 2008;13:5732–54.
[31] Goel A, Vogel V. Harnessing biological motors to engineer systems for nanoscale transport and assembly. Nat Nanotechnol 2008;3:465–75.
[32] Fulga F, Nicolau Jr DV. Models of protein linear molecular motors for dynamic nanodevices. Integr Biol 2009;1:150–69.
[33] Spetzler D, York J, Dobbin C, Martin J, Ishmukhametov R, Day L, et al. Recent developments of bio-molecular motors as on-chip devices using single molecule techniques. Lab Chip 2007;7:1633–43.
[34] Howard J. Mechanics of motor proteins and the cytoskeleton. Sunderland, MA: Sinauer; 2001.
[35] Alberts B, Johnson A, Lewis J, Raff M, Roberts K, Walter P. Molecular biology of the cell. 4th ed. New York: Garland; 2002.
[36] Maniotis AJ, Chen CS, Ingber DE. Demonstration of mechanical connections between integrins, cytoskeletal filaments, and nucleoplasm that stabilize nuclear structure. Proc Natl Acad Sci USA 1997;94:849–54.
[37] Thomas DD, dos Remedios CG. Results and problems in cell differentiation. Molecular interactions of actin: actin–myosin interaction and actin-based regulation. New York: Springer–Verlag; 2002.
[38] Kabsch W, Vandekerckhove J. Structure and function of actin. Annu Rev Biophys Biomol Struct 1992;21:49–76.
[39] Mitchison TJ, Cramer LP. Actin-based cell motility and cell locomotion. Cell 1996;84:371–9.
[40] Nogales E. Structural insights into microtubule function. Annu Rev Biochem 2000;69:277–302.
[41] Mitchison T, Kirschner M. Microtubule assembly nucleated by isolated centrosomes. Nature 1984;312:232–7.
[42] Brangwynne CP, MacKintosh FC, Kumar S, Geisse NA, Talbot J, Mahadevan L, et al. Microtubules can bear enhanced compressive loads in living cells because of lateral reinforcement. J Cell Biol 2006;173:733–41.
[43] Goldman RD, Grin B, Mendez MG, Kuczmarski ER. Intermediate filaments: versatile building blocks of cell structure. Curr Opin Cell Biol 2008;20:28–34.
[44] Holmes KC, Popp D, Gebhard W, Kabsch W. Atomic model of the actin filament. Nature 1990;347:44–8.
[45] Cooper JA. Effects of cytochalasin and phalloidin on actin. J Cell Biol 1987;105:1473–8.
[46] Vikhorev PG, Vikhoreva NN, Sundberg M, Balaz M, Albet-Torres N, Bunk R, et al. Diffusion dynamics of motor-driven transport: gradient production and self-organization of surfaces. Langmuir 2008;24:13509–17.
[47] Nitta T, Tanahashi A, Obara Y, Hirano M, Razumova M, Regnier M, et al. Comparing guiding track requirements for myosin- and kinesin-powered molecular shuttles. Nano Lett 2008;8:2305–9.
[48] Vikhorev PG, Vikhoreva NN, Månsson A. Bending flexibility of actin filaments during motor-induced sliding. Biophys J 2008;95:5809–19.
[49] Nogales E, Wolf SG, Downing KH. Structure of the alpha beta tubulin dimer by electron crystallography. Nature 1998;391:199–203.
[50] Kozielski F, Sack S, Marx A, Thormahlen M, Schonbrunn E, Biou V, et al. The crystal structure of dimeric kinesin and implications for microtubule-dependent motility. Cell 1997;91:985–94.
[51] Li HL, DeRosier DJ, Nicholson WV, Nogales E, Downing KH. Microtubule structure at 8 angstrom resolution. Structure 2002;10:1317–28.
[52] Chretien D, Metoz F, Verde F, Karsenti E, Wade RH. Lattice defects in microtubules: protofilament numbers vary within individual microtubules. J Cell Biol 1992;117:1031–40.
[53] Mitchison T, Kirschner M. Dynamic instability of microtubule growth. Nature 1984;312:237–42.
[54] Nogales E, Whittaker M, Milligan RA, Downing KH. High-resolution model of the microtubule. Cell 1999;96:79–88.
[55] Dimitrov A, Quesnoit M, Moutel S, Cantaloube I, Pous C, Perez F. Detection of GTP-tubulin conformation in vivo reveals a role for GTP remnants in microtubule rescues. Science 2008;322:1353–6.
[56] Nogales E, Wang H-W. Structural mechanisms underlying nucleotide-dependent self-assembly of tubulin and its relatives. Curr Opin Struct Biol 2006;16:221–9.
[57] Wang H-W, Nogales E. Nucleotide-dependent bending flexibility of tubulin regulates microtubule assembly. Nature 2005;435:911–5.
[58] Dogterom M, Kerssemakers JWJ, Romet-Lemonne G, Janson ME. Force generation by dynamic microtubules. Curr Opin Cell Biol 2005;17:67–74.
[59] Westermann S, Wang H-W, Avila-Sakar A, Drubin DG, Nogales E, Barnes G. The Dam1 kinetochore ring complex moves pro-

cessively on depolymerizing microtubule ends. Nature 2006;440:565–9.
[60] Howard J. Elastic and damping forces generated by confined arrays of dynamic microtubules. Phys Biol 2006;3:54–66.
[61] Davis LJ, Odde DJ, Block SM, Gross SP. The importance of lattice defects in katanin-mediated microtubule severing in vitro. Biophys J 2002;82:2916–27.
[62] Bouchard AM, Warrender CE, Osbourn GC. Harnessing microtubule dynamic instability for nanostructure assembly. Phys Rev E 2006;74:041902.
[63] Patolsky F, Weizmann Y, Willner I. Actin-based metallic nanowires as bio-nanotransporters. Nat Mater 2004;3:692–5.
[64] Behrens S, Rahn K, Habicht W, Böhm K-J, Rösner H, Dinjus E, et al. Nanoscale particle arrays induced by highly ordered protein assemblies. Adv Mater 2002;14:1621–5.
[65] Behrens S, Wu J, Habicht W, Unger E. Silver nanoparticle and nanowire formation by microtubule templates. Chem Mater 2004;16:3085–90.
[66] Behrens S, Habicht W, Wu J, Unger E. Tubulin assemblies as biomolecular templates for nanostructure synthesis: from nanoparticle arrays to nanowires. Surf Interface Anal 2006;38:1014–8.
[67] Tucker R, Katira P, Hess H. Herding nanotransporters: localized activation via release and sequestration of control molecules. Nano Lett 2008;8:221–6.
[68] Spoerke ED, Bachand GD, Liu J, Sasaki D, Bunker BC. Directing the polar organization of microtubules. Langmuir 2008;24:7039–43.
[69] Hyman AA, Drechsel DN, Kellog D, Salser S, Sawin K, Steffen P, et al. Preparation of modified tubulins. Meth Enzymol 1991;196:478–85.
[70] Peloquin J, Komarova Y, Borisy G. Conjugation of fluorophores to tubulin. Nat Meth 2005;2:299–303.
[71] Schiff PB, Fant J, Horwitz SB. Promotion of microtubule assembly in vitro by taxol. Nature 1979;277:665–7.
[72] Turner D, Chang C, Fang K, Cuomo P, Murphy D. Kinesin movement on glutaraldehyde-fixed microtubules. Anal Biochem 1996;242:20–5.
[73] Boal AK, Tellez H, Rivera SB, Miller NE, Bachand GD, Bunker BC. The stability and functionality of chemically crosslinked microtubules. Small 2006;2:793–803.
[74] Boal AK, Headley TJ, Tissot RG, Bunker BC. Microtubule-templated biomimetic mineralization of lepidocrocite. Adv Funct Mater 2004;14:19–24.
[75] Dinu CZ, Bale SS, Zhu GY, Dordick JS. Tubulin encapsulation of carbon nanotubes into functional hybrid assemblies. Small 2009;5:310–5.
[76] Oster G, Wang HY. Rotary protein motors. Trends Cell Biol 2003;13:114–21.
[77] Schliwa M, Woehlke G. Molecular motors. Nature 2003;422:759–65.
[78] Case RB, Rice S, Hart CL, Ly B, Vale RD. Role of the kinesin neck linker and catalytic core in microtubule-based motility. Curr Biol 2000;10:157–60.
[79] Wu XS, Rao K, Zhang H, Wang F, Sellers JR, Matesic LE, et al. Identification of an organelle receptor for myosin-Va. Nat Cell Biol 2002;4:271–8.
[80] Mermall V, Post PL, Mooseker MS. Unconventional myosins in cell movement, membrane traffic, and signal transduction. Science 1998;279:527–33.
[81] Geli MI, Riezman H. Role of type I myosins in receptor-mediated endocytosis in yeast. Science 1996;272:533–5.
[82] Schott DH, Collins RN, Bretscher A. Secretory vesicle transport velocity in living cells depends on the myosin-V lever arm length. J Cell Biol 2002;156:35–40.
[83] Kros CJ, Marcotti W, van Netten SM, Self TJ, Libby RT, Brown SDM, et al. Reduced climbing and increased slipping adaptation in cochlear hair cells of mice with Myo7a mutations. Nat Neurosci 2002;5:41–7.
[84] Huxley HE. Mechanism of muscular contraction. Science 1969;164:1356–66.
[85] Huxley AF, Simmons RM. Proposed mechanism of force generation in striated muscle. Nature 1971;233:533–8.
[86] Rayment I, Holden HM, Whittaker M, Yohn CB, Lorenz M, Holmes KC, et al. Structure of the actin–myosin complex and its implications for muscle contraction. Science 1993;261:58–65.
[87] Foth BJ, Goedecke MC, Soldati D. New insights into myosin evolution and classification. Proc Natl Acad Sci USA 2006;103:3681–6.
[88] Asokan SB, Jawerth L, Carroll RL, Cheney RE, Washburn S, Superfine R. Two-dimensional manipulation and orientation of actin–myosin systems with dielectrophoresis. Nano Lett 2003;3:431–7.
[89] Uyeda TQP, Kron SJ, Spudich JA. Myosin step size: estimation from slow sliding movement of actin over low densities of heavy meromyosin. J Mol Biol 1990;214:699–710.
[90] De La Cruz EM, Wells AL, Rosenfeld SS, Ostap EM, Sweeney HL. The kinetic mechanism of myosin V. Proc Natl Acad Sci USA 1999;96:13726–31.
[91] Vale RD, Milligan RA. The way things move: looking under the hood of molecular motor proteins. Science 2000;288:88–95.
[92] Harada Y, Sakurada K, Aoki T, Thomas DD, Yanagida T. Mechanochemical coupling in actomyosin energy transduction studied by in vitro movement assay. J Mol Biol 1990;216:49–68.
[93] Astumian RD. Thermodynamics and kinetics of a Brownian motor. Science 1997;276:917–22.
[94] Block SM. Kinesin motor mechanics: binding, stepping, tracking, gating, and limping. Biophys J 2007;92:2986–95.
[95] Hirokawa N, Takemura R. Kinesin superfamily proteins and their various functions and dynamics. Exp Cell Res 2004;301:50–9.
[96] Gunawardena S, Goldstein LSB. Cargo-carrying motor vehicles on the neuronal highway: transport pathways and neurodegenerative disease. J Neurobiol 2004;58:258–71.
[97] Sharp DJ, Rogers GC, Scholey JM. Microtubule motors in mitosis. Nature 2000;407:41–7.
[98] Insinna C, Besharse JC. Intraflagellar transport and the sensory outer segment of vertebrate photoreceptors. Dev Dynam 2008;237:1982–92.
[99] Hirokawa N, Pfister KK, Yorifuji H, Wagner MC, Brady ST, Bloom GS. Submolecular domains of bovine brain kinesin identified by electron microscopy and monoclonal antibody decoration. Cell 1989;56:867–78.
[100] Asbury CL. Kinesin: world's tiniest biped. Curr Opin Cell Biol 2005;17:89–97.
[101] Coy DL, Wagenbach M, Howard J. Kinesin takes one 8-nm step for each ATP that it hydrolyzes. J Biol Chem 1999;274:3667–71.
[102] Hancock WO, Howard J. Kinesin's processivity results from mechanical and chemical coordination between the ATP hydrolysis cycles of the two motor domains. Proc Natl Acad Sci USA 1999;96:13147–52.
[103] Coy DL, Hancock WO, Wagenbach M, Howard J. Kinesin's tail domain is an inhibitory regulator of the motor domain. Nat Cell Biol 1999;1:288–92.
[104] Howard J, Hudspeth AJ, Vale RD. Movement of microtubules by single kinesin molecules. Nature 1989;342:154–8.
[105] Yanagida T, Nakase M, Nishiyama K, Oosawa F. Direct observation of motion of single F-actin filaments in the presence of myosin. Nature 1984;307:58–60.
[106] Kron SJ, Spudich JA. Fluorescent actin filaments move on myosin fixed to a glass surface. Proc Natl Acad Sci USA 1986;83:6272–6.
[107] Kron SJ, Toyoshima YY, Uyeda TQP, Spudich JA. Assays for actin sliding movement over myosin-coated surfaces. Meth Enzymol 1991;196:399–416.
[108] Howard J, Hunt AJ, Baek S. Assay of microtubule movement driven by single kinesin molecules. Methods Cell Biol 1993;39:137–47.
[109] Yildiz A, Forkey JN, McKinney SA, Ha T, Goldman YE, Selvin PR, et al. Myosin V walks hand-over-hand: single fluorophore imaging with 1.5-nm localization. Science 2003;300:2061–5.
[110] Yildiz A, Tomishige M, Vale RD, Selvin PR. Kinesin walks hand-over-hand. Science 2004;303:676–8.
[111] Reck-Peterson SL, Yildiz A, Carter AP, Gennerich A, Zhang N, Vale RD. Single-molecule analysis of dynein processivity and stepping behavior. Cell 2006;126:335–48.
[112] Svoboda K, Schmidt CF, Schnapp BJ, Block SM. Direct observation of kinesin stepping by optical trapping interferometry. Nature 1993;365:721–7.
[113] Finer JT, Simmons RM, Spudich JA. Single myosin molecule mechanics: piconewton forces and nanometre steps. Nature 1994;368:113–9.
[114] Sakakibara H, Kojima H, Sakai Y, Katayama E, Oiwa K. Inner-arm dynein c of *Chlamydomonas* flagella is a single-headed processive motor. Nature 1999;400:586–90.
[115] Kerssemakers JWJ, Laura Munteanu E, Laan L, Noetzel TL, Janson ME, Dogterom M. Assembly dynamics of microtubules at molecular resolution. Nature 2006;442:709–12.
[116] Arai Y, Yasuda R, Akashi K-I, Harada Y, Miyata H, Kinosita K, et al. Tying a molecular knot with optical tweezers. Nature 1999;399:446–8.
[117] Visscher K, Schnitzer MJ, Block SM. Single kinesin molecules studied with a molecular force clamp. Nature 1999;400:184–9.
[118] Klumpp S, Lipowsky R. Cooperative cargo transport by several molecular motors. Proc Natl Acad Sci USA 2005;102:17284–9.

[119] Mueller MJI, Klumpp S, Lipowsky R. Tug-of-war as a cooperative mechanism for bidirectional cargo transport by molecular motors. Proc Natl Acad Sci USA 2008;105:4609–14.
[120] Visscher K, Gross SP, Block SM. Construction of multiple-beam optical traps with nanometer-resolution position sensing. IEEE J Selected Top Quantum Electron 1996;2:1066–76.
[121] Vanzi F, Capitanio M, Sacconi L, Stringari C, Cicchi R, Canepari M, et al. New techniques in linear and non-linear laser optics in muscle research. J Muscle Res Cell Motility 2006;27:469–79.
[122] Doot RK, Hess H, Vogel V. Engineered networks of oriented microtubule filaments for directed cargo transport. Soft Matter 2007;3:349–56.
[123] Katira P, Agarwal A, Fischer T, Chen H-Y, Jiang X, Lahann J, et al. Quantifying the performance of protein-resisting surfaces at ultra-low protein coverages using kinesin motor proteins as probes. Adv Mater 2007;19:3171–6.
[124] Berliner E, Mahtani HK, Karki S, Chu LF, Cronan JE, Gelles J. Microtubule movement by a biotinated kinesin bound to a strepavidin-coated surface. J Biol Chem 1994;269:8610–5.
[125] Yu T, Wang Q, Johnson DS, Wang MD, Ober CK. Functional hydrogel surfaces: binding kinesin-based molecular motor proteins to selected patterned sites. Adv Funct Mater 2005;15:1303–9.
[126] Leduc C, Ruhnow F, Howard J, Diez S. Detection of fractional steps in cargo movement by the collective operation of kinesin-1 motors. Proc Natl Acad Sci USA 2007;104:10847–52.
[127] Kerssemakers J, Ionov L, Queitsch U, Luna S, Hess H, Diez S. 3D nanometer tracking of motile microtubules on reflective surfaces. Small 2009;5:1732–7.
[128] Kerssemakers J, Howard J, Hess H, Diez S. The distance that kinesin holds its cargo from the microtubule surface measured by fluorescence-interference-contrast microscopy. Proc Natl Acad Sci USA 2006;103:15812–7.
[129] Goldstein LS, Philp AV. The road less traveled: emerging principles of kinesin motor utilization. Annu Rev Cell Dev Biol 1999;15:141–83.
[130] Dennis JR, Howard J, Vogel V. Molecular shuttles: directed motion of microtubules along nanoscale kinesin tracks. Nanotechnology 1999;10:232–6.
[131] Hess H, Clemmens J, Qin D, Howard J, Vogel V. Light-controlled molecular shuttles made from motor proteins carrying cargo on engineered surfaces. Nano Lett 2001;1:235–9.
[132] Fischer T, Agarwal A, Hess H. A smart dust biosensor powered by kinesin motors. Nat Nanotechnol 2009;4:162–6.
[133] Sheehan PE, Whitman LJ. Detection limits for nanoscale biosensors. Nano Lett 2005;5:803–7.
[134] Turner DC, Chang CY, Fang K, Brandow SL, Murphy DB. Selective adhesion of functional microtubules to patterned silane surfaces. Biophys J 1995;69:2782–9.
[135] Limberis L, Stewart RJ. Toward kinesin-powered microdevices. Nanotechnology 2000;11:47–51.
[136] Limberis L, Stewart RJ. Polarized alignment and surface immobilization of microtubules for kinesin-powered nanodevices. Nano Lett 2001;1:277–80.
[137] Brown TB, Hancock WO. A polarized microtubule array for kinesin-powered nanoscale assembly and force generation. Nano Lett 2002;2:1131–5.
[138] Muthukrishnan G, Roberts CA, Chen YC, Zahn JD, Hancock WO. Patterning surface-bound microtubules through reversible DNA hybridization. Nano Lett 2004;4:2127–32.
[139] Interliggi KA, Zeile WL, Ciftan-Hens SA, McGuire GE, Purich DL, Dickinson RB. Guidance of actin filament elongation on filament-binding tracks. Langmuir 2007;23:11911–6.
[140] Böhm KJ, Stracke R, Mühlig P, Unger E. Motor protein-driven unidirectional transport of micrometer-sized cargoes across isopolar microtubule arrays. Nanotechnology 2001;12:238–44.
[141] Yokokawa R, Takeuchi S, Kon T, Ohkura RAOR, Edamatsu MAEM, Sutoh KASK, et al. Transportation of micromachined structures by biomolecular linear motors. In: Takeuchi S, editor. Microelectro mechanical systems. Kyoto: IEEE; 2003. p. 8.
[142] Yokokawa R, Takeuchi S, Kon T, Nishiura M, Sutoh K, Fujita H. Unidirectional transport of kinesin-coated beads on microtubules oriented in a microfluidic device. Nano Lett 2004;4:2265–70.
[143] Bohm KJ, Beeg J, Meyer zu Horste G, Stracke RASR, Unger EAUE. Kinesin-driven sorting machine on large-scale microtubule arrays. Adv Packaging IEEE Trans 2005;28:571–6 [see also Comp Packaging Manuf Technol, Part B: Adv Packaging, IEEE Trans].
[144] Yokokawa R, Yoshida Y, Takeuchi S, Kon T, Fujita H. Unidirectional transport of a bead on a single microtubule immobilized in a sub-micrometre channel. Nanotechnology 2006;17:289–94.
[145] Muthukrishnan G, Hutchins BM, Williams ME, Hancock WO. Transport of semiconductor nanocrystals by kinesin molecular motors. Small 2006;2:626–30.
[146] Yokokawa R, Tarhan MC, Kon T, Fujita H. Simultaneous and bidirectional transport of kinesin-coated microspheres and dynein-coated microspheres on polarity-oriented microtubules. Biotechnol Bioeng 2008;101:1–8.
[147] Song WX, He Q, Cui Y, Mohwald H, Diez S, Li JB. Assembled capsules transportation driven by motor proteins. Biochem Biophys Res Commun 2009;379:175–8.
[148] Bottier C, Fattaccioli J, Tarhan MC, Yokokawa R, Morin FO, Kim B, et al. Active transport of oil droplets along oriented microtubules by kinesin molecular motors. Lab Chip 2009;9:1694–700.
[149] Nitta T, Hess H. Dispersion in active transport by kinesin-powered molecular shuttles. Nano Lett 2005;5:1337–42.
[150] Katira P, Hess H. Two-stage capture employing active transport enables sensitive and fast biosensors, submitted to Nano Letters.
[151] Clemmens J, Hess H, Lipscomb R, Hanein Y, Boehringer KF, Matzke CM, et al. Mechanisms of microtubule guiding on microfabricated kinesin-coated surfaces: chemical and topographic surface patterns. Langmuir 2003;19:10967–74.
[152] Sundberg M, Bunk R, Albet-Torres N, Kvennefors A, Persson F, Montelius L, et al. Actin filament guidance on a chip: toward high-throughput assays and lab-on-a-chip applications. Langmuir 2006;22:7286–95.
[153] Suzuki H, Oiwa K, Yamada A, Sakakibara H, Nakayama H, Mashiko S. Linear arrangement of motor protein on a mechanically deposited fluoropolymer thin film. Jpn J Appl Phys Part 1 1995;34:3937–41.
[154] Stracke P, Bohm KJ, Burgold J, Schacht HJ, Unger E. Physical and technical parameters determining the functioning of a kinesin-based cell-free motor system. Nanotechnology 2000;11:52–6.
[155] Clemmens J, Hess H, Howard J, Vogel V. Analysis of microtubule guidance in open microfabricated channels coated with the motor protein kinesin. Langmuir 2003;19:1738–44.
[156] Hiratsuka Y, Tada T, Oiwa K, Kanayama T, Uyeda TQ. Controlling the direction of kinesin-driven microtubule movements along microlithographic tracks. Biophys J 2001;81:1555–61.
[157] Hess H, Clemmens J, Matzke CM, Bachand GD, Bunker BC, Vogel V. Ratchet patterns sort molecular shuttles. Appl Phys A 2002;75:309–13.
[158] Lin C-T, Kao M-T, Kurabayashi K, Meyhöfer E. Efficient designs for powering microscale devices with nanoscale biomolecular motors. Small 2006;2:281–7.
[159] Nitta T, Tanahashi A, Hirano M, Hess H. Simulating molecular shuttle movements: towards computer-aided design of nanoscale transport systems. Lab Chip 2006;6:881–5.
[160] Hess H, Matzke CM, Doot RK, Clemmens J, Bachand GD, Bunker BC, et al. Molecular shuttles operating undercover: a new photolithographic approach for the fabrication of structured surfaces supporting directed motility. Nano Lett 2003;3:1651–5.
[161] Bunk R, Sundberg M, Mansson A, Nicholls IA, Omling P, Tagerud S, et al. Guiding motor-propelled molecules with nanoscale precision through silanized bi-channel structures. Nanotechnology 2005;16:710–7.
[162] Clemmens J, Hess H, Doot R, Matzke CM, Bachand GD, Vogel V. Motor-protein "roundabouts": microtubules moving on kinesin-coated tracks through engineered networks. Lab Chip 2004;4:83–6.
[163] Huang YM, Uppalapati M, Hancock WO, Jackson TN. Microfabricated capped channels for biomolecular motor-based transport. IEEE Trans Adv Packaging 2005;28:564–70.
[164] Huang YM, Uppalapati M, Hancock WO, Jackson TN. Microtubule transport, concentration and alignment in enclosed microfluidic channels. Biomed Microdev 2007;9:175–84.
[165] van den Heuvel MGL, De Graaff MP, Dekker C. Molecular sorting by electrical steering of microtubules in kinesin-coated channels. Science 2006;312:910–4.
[166] Hunt AJ, Howard J. Kinesin swivels to permit microtubule movement in any direction. Proc Natl Acad Sci USA 1993;90:11653–7.
[167] Suzuki H, Yamada A, Oiwa K, Nakayama H, Mashiko S. Control of actin moving trajectory by patterned poly(methylmethacrylate) tracks. Biophys J 1997;72:1997–2001.
[168] Nicolau DV, Suzuki H, Mashiko S, Taguchi T, Yoshikawa S. Actin motion on microlithographically functionalized myosin surfaces and tracks. Biophys J 1999;77:1126–34.
[169] Sundberg M, Rosengren JP, Bunk R, Lindahl J, Nicholls IA, Tagerud S, et al. Silanized surfaces for in vitro studies of actomyosin function and nanotechnology applications. Anal Biochem 2003;323:127–38.
[170] Sundberg M, Balaz M, Bunk R, Rosengren-Holmberg JP, Montelius L, Nicholls IA, et al. Selective spatial localization of

actomyosin motor function by chemical surface patterning. Langmuir 2006;22:7302–12.
[171] Albet-Torres N, O'Mahony J, Charlton C, Balaz M, Lisboa P, Aastrup T, et al. Mode of heavy meromyosin adsorption and motor function correlated with surface hydrophobicity and charge. Langmuir 2007;23:11147–56.
[172] Lipscomb RC, Clemmens J, Hanein Y, Holl MR, Vogel V, Ratner BD, et al. Controlled microtubules transport on patterned. Non-adhesive surfaces. In: Second international IEEE-EMBS special topic conference on microtechnologies in medicine & biology. 2002. p. 21.
[173] Manandhar P, Huang L, Grubich JR, Hutchinson JW, Chase PB, Hong SH. Highly selective directed assembly of functional actomyosin on Au surfaces. Langmuir 2005;21:3213–6.
[174] Romet-Lemonne G, VanDuijn M, Dogterom M. Three-dimensional control of protein patterning in microfabricated devices. Nano Lett 2005;5:2350–4.
[175] Byun KE, Kim MG, Chase PB, Hong SH. Selective assembly and guiding of actomyosin using carbon nanotube network monolayer patterns. Langmuir 2007;23:9535–9.
[176] Yano Toyoshima Y, Toyoshima C, Spudich JA. Bidirectional movement of actin filaments along tracks of myosin heads. Nature 1989;341:154–6.
[177] Reuther C, Hajdo L, Tucker R, Kasprzak AA, Diez S. Biotemplated nanopatterning of planar surfaces with molecular motors. Nano Lett 2006;6:2177–83.
[178] Cheng LJ, Kao MT, Meyhofer E, Guo LJ. Highly efficient guiding of microtubule transport with imprinted CYTOP nanotracks. Small 2005;1:409–14.
[179] Moorjani SG, Jia L, Jackson TN, Hancock WO. Lithographically patterned channels spatially segregate kinesin motor activity and effectively guide microtubule movements. Nano Lett 2003;3:633–7.
[180] Jia L, Moorjani SG, Jackson TN, Hancock WO. Microscale transport and sorting by kinesin molecular motors. Biomed Microdev 2004;6:67–74.
[181] van den Heuvel MG, Butcher CT, Smeets RM, Diez S, Dekker C. High rectifying efficiencies of microtubule motility on kinesin-coated gold nanostructures. Nano Lett 2005;5:1117–22.
[182] Boal AK, Bauer JM, Rivera SB, Manley RG, Manginell RP, Bachand GD, et al. Monolayer engineered microchannels for motor protein transport platforms. Polym Preprints 2004;45:96–7.
[183] Mahanivong C, Wright JP, Kekic M, Pham DK, dos Remedios C, Nicolau DV. Manipulation of the motility of protein molecular motors on microfabricated substrates. Biomed Microdev 2002;4:111–6.
[184] Wright J, Pham D, Mahanivong C, Nicolau DV, Kekic M, dos Remedios CG. Micropatterning of myosin on O-acryloyl acetophenone oxime (AAPO), layered with bovine serum albumin (BSA). Biomed Microdev 2002;4:205–11.
[185] Jaber JA, Chase PB, Schlenoff JB. Actomyosin-driven motility on patterned polyelectrolyte mono- and multilayers. Nano Lett 2003;3:1505–9.
[186] Bunk R, Klinth J, Montelius L, Nicholls IA, Omling P, Tagerud S, et al. Actomyosin motility on nanostructured surfaces. Biochem Biophys Res Commun 2003;301:783–8.
[187] Bunk R, Klinth J, Rosengren J, Nicholls I, Tagerud S, Omling P, et al. Towards a 'nano-traffic' system powered by molecular motors. Microelectro Eng 2003;67-8:899–904.
[188] Bunk R, Carlberg P, Mansson A, Nicholls IA, Omling P, Sundberg M, et al. Guiding molecular motors with nano-imprinted structures. Jpn J App Phys Part 1 2005;44:3337–40.
[189] Fritzsche W, Bohm K, Unger E, Kohler JM. Making electrical contact to single molecules. Nanotechnology 1998;9:177–83.
[190] Ostap EM, Yanagida T, Thomas DD. Orientational distribution of spin-labeled actin oriented by flow. Biophys J 1992;63:966–75.
[191] Yokokawa R, Murakami T, Sugie T, Kon T. Polarity orientation of microtubules utilizing a dynein-based gliding assay. Nanotechnology 2008;19, 125505/1–7.
[192] Kim T, Kao MT, Meyhofer E, Hasselbrink EF. Biomolecular motor-driven microtubule translocation in the presence of shear flow: analysis of redirection behaviours. Nanotechnology 2007;18, 025101/1–9.
[193] Brunner C, Hess H, Ernst K-H, Vogel V. Lifetime of biomolecules in hybrid nanodevices. Nanotechnology 2004;15:S540–8.
[194] Riveline D, Ott A, Julicher F, Winkelmann DA, Cardoso O, Lacapere JJ, et al. Acting on actin: the electric motility assay. Eur Biophys J 1998;27:403–8.
[195] Stracke R, Bohm KJ, Wollweber L, Tuszynski JA, Unger E. Analysis of the migration behaviour of single microtubules in electric fields. Biochem Biophys Res Commun 2002;293:602–9.
[196] Kim T, Kao MT, Hasselbrink EF, Meyhofer E. Active alignment of microtubules with electric fields. Nano Lett 2007;7:211–7.
[197] Kim T, Kao MT, Hasselbrink EF, Meyhofer E. Nanomechanical model of microtubule translocation in the presence of electric fields. Biophys J 2008;94:3880–92.
[198] Bras W, Diakun GP, Diaz JF, Maret G, Kramer H, Bordas J, et al. The susceptibility of pure tubulin to high magnetic fields: a magnetic birefringence and X-ray fiber diffraction study. Biophys J 1998;74:1509–21.
[199] Platt M, Hancock WO, Muthukrishnan G, Williams ME. Millimeter scale alignment of magnetic nanoparticle functionalized microtubules in magnetic fields. J Am Chem Soc 2005;127:15686–7.
[200] Hutchins BM, Hancock WO, Williams ME. Magnet assisted fabrication of microtubule arrays. Phys Chem Chem Phys 2006;8:3507–9.
[201] Hutchins BM, Platt M, Hancock WO, Williams ME. Directing transport of $CoFe_2O_4$-functionalized microtubules with magnetic fields. Small 2007;3:126–31.
[202] Holohan SJP, Marston SB. Force–velocity relationship of single actin filament interacting with immobilised myosin measured by electromagnetic technique. IEE Proc Nanobiotechnol 2005;152:113–20.
[203] van den Heuvel MGL, Bolhuis S, Dekker C. Persistence length measurements from stochastic single-microtubule trajectories. Nano Lett 2007;7:3138–44.
[204] van den Heuvel MGL, de Graaff MR, Dekker C. Microtubule curvatures under perpendicular electric forces reveal a low persistence length. Proc Natl Acad Sci USA 2008;105:7941–6.
[205] Hirokawa N, Takemura R. Molecular motors and mechanisms of directional transport in neurons. Nat Rev Neurosci 2005;6:201–14.
[206] Sase I, Miyata H, Ishiwata S, Kinosita K. Axial rotation of sliding actin filaments revealed by single-fluorophore imaging. Proc Natl Acad Sci USA 1997;94:5646–50.
[207] Beausang JF, Schroeder HW, Nelson PC, Goldman YE. Twirling of actin by myosins II and V observed via polarized TIRF in a modified gliding assay. Biophys J 2008;95:5820–31.
[208] Ray S, Meyhofer E, Milligan RA, Howard J. Kinesin follows the microtubule's protofilament axis. J Cell Biol 1993;121:1083–93.
[209] Nitzsche B, Ruhnow F, Diez S. Quantum-dot-assisted characterization of microtubule rotations during cargo transport. Nat Nanotechnol 2008;3:552–6.
[210] Bachand GD, Rivera SB, Boal AK, Gaudioso J, Liu J, Bunker BC. Assembly and transport of nanocrystal CdSe quantum dot nanocomposites using microtubules and kinesin motor proteins. Nano Lett 2004;4:817–21.
[211] Korten T, Diez S. Setting up roadblocks for kinesin-1: mechanism for the selective speed control of cargo carrying microtubules. Lab Chip 2008;8:1441–7.
[212] Bachand M, Trent AM, Bunker BC, Bachand GD. Physical factors affecting kinesin-based transport of synthetic nanoparticle cargo. J Nanosci Nanotechnol 2005;5:718–22.
[213] Brunner C, Wahnes C, Vogel V. Cargo pick-up from engineered loading stations by kinesin driven molecular shuttles. Lab Chip 2007;7:1263–71.
[214] Agarwal A, Katira P, Hess H. Millisecond curing time of a molecular adhesive causes velocity-dependent cargo-loading of molecular shuttles. Nano Lett 2009;9:1170–5.
[215] Ramachandran S, Ernst K-H, Bachand GD, Vogel V, Hess H. Selective loading of kinesin-powered molecular shuttles with protein cargo and its application to biosensing. Small 2006;2:330–4.
[216] Hess H, Clemmens J, Brunner C, Doot R, Luna S, Ernst K-H, et al. Molecular self-assembly of "nanowires" and "nanospools" using active transport. Nano Lett 2005;5:629–33.
[217] Hess H. Self-assembly driven by molecular motors. Soft Matter 2006;2:669–77.
[218] Liu HQ, Spoerke ED, Bachand M, Koch SJ, Bunker BC, Bachand GD. Biomolecular motor-powered self-assembly of dissipative nanocomposite rings. Adv Mater 2008;20:4476–81.
[219] Kawamura R, Kakugo A, Shikinaka K, Osada Y, Gong JP. Ring-shaped assembly of microtubules shows preferential counterclockwise motion. Biomacromolecules 2008;9:2277–82.
[220] Hiyama S, Gojo R, Shima T, Takeuchi S, Sutoh K. Biomolecular-motor-based nano- or microscale particle translocations on DNA microarrays. Nano Lett 2009;9:2407–13.
[221] Diez S, Reuther C, Dinu C, Seidel R, Mertig M, Pompe W, et al. Stretching and transporting DNA molecules using motor proteins. Nano Lett 2003;3:1251–4.
[222] Dinu CZ, Opitz J, Pompe W, Howard J, Mertig M, Diez S. Parallel manipulation of bifunctional DNA molecules on structured surfaces using kinesin-driven microtubules. Small 2006;2:1090–8.

[223] Yokokawa R, Miwa J, Tarhan MC, Fujita H, Kasahara M. DNA molecule manipulation by motor proteins for analysis at the single-molecule level. Anal Bioanal Chem 2008;391:2735–43.
[224] Taira S, Du YZ, Hiratsuka Y, Konishi K, Kubo T, Uyeda TQP, et al. Selective detection and transport of fully matched DNA by DNA-loaded microtubule and kinesin motor protein. Biotechnol Bioeng 2006;95:533–8.
[225] Dinu CZ, Bale SS, Chrisey DB, Dordick JS. Manipulation of individual carbon nanotubes by reconstructing the intracellular transport of a living cell. Adv Mater 2009;21:1182–6.
[226] Raab M, Hancock WO. Transport and detection of unlabeled nucleotide targets by microtubules functionalized with molecular beacons. Biotechnol Bioeng 2008;99:764–73.
[227] Bachand GD, Rivera SB, Carroll-Portillo A, Hess H, Bachand M. Active capture and transport of virus particles using a biomolecular motor-driven, nanoscale antibody sandwich assay. Small 2006;2:381–5.
[228] Martin BD, Soto CM, Blum AS, Sapsford KE, Whitley JL, Johnson JE, et al. An engineered virus as a bright fluorescent tag and scaffold for cargo proteins—capture and transport by gliding microtubules. J Nanosci Nanotechnol 2006;6:2451–60.
[229] Soto CM, Martin BD, Sapsford KE, Blum AS, Ratna BR. Toward single molecule detection of Staphylococcal enterotoxin B: mobile sandwich immunoassay on gliding microtubules. Anal Chem 2008;80:5433–40.
[230] Rios L, Bachand GD. Multiplex transport and detection of cytokines using kinesin-driven molecular shuttles. Lab Chip 2009;9:1005–10.
[231] Hirabayashi M, Taira S, Kobayashi S, Konishi K, Katoh K, Hiratsuka Y, et al. Malachite green-conjugated microtubules as mobile bioprobes selective for malachite green aptamers with capturing/releasing ability. Biotechnol Bioeng 2006;94:473–80.
[232] Hiyama S, Inoue T, Shima T, Moritani Y, Suda T, Sutoh K. Autonomous loading, transport, and unloading of specified cargoes by using DNA hybridization and biological motor-based motility. Small 2008;4:410–5.
[233] Du YZ, Hiratsuka Y, Taira S, Eguchi M, Uyeda TQP, Yumoto N, et al. Motor protein nano-biomachine powered by self-supplying ATP. Chem Commun 2005:2080–2.
[234] Kato KA, Goto R, Katoh K, Shibakami M. Microtubule–cyclodextrin conjugate: functionalization of motile filament with molecular inclusion ability. Biosci Biotechnol Biochem 2005;69:646–8.
[235] Suzuki N, Miyata H, Ishiwata S, Kinoshita K. Preparation of bead-tailed actin filaments: estimation of the torque produced by the sliding force in an in vitro motility assay. Biophys J 1996;70:401–8.
[236] Kaur H, Das T, Kumar R, Ajore R, Bharadwaj LA. Covalent attachment of actin filaments to Tween 80 coated polystyrene beads for cargo transportation. Biosystems 2008;92:69–75.
[237] Mansson A, Sundberg M, Balaz M, Bunk R, Nicholls IA, Omling P, et al. In vitro sliding of actin filaments labelled with single quantum dots. Biochem Biophys Res Commun 2004;314:529–34.
[238] Lin CT, Kao MT, Kurabayashi K, Meyhofer E. Self-contained biomolecular motor-driven protein sorting and concentrating in an ultrasensitive microfluidic chip. Nano Lett 2008;8:1041–6.
[239] Taira S, Du YZ, Hiratsuka Y, Uyeda TQP, Yumoto N, Kodaka M. Loading and unloading of molecular cargo by DNA-conjugated microtubule. Biotechnol Bioeng 2008;99:734–9.
[240] Boal AK, Bachand GD, Rivera SB, Bunker BC. Interactions between cargo-carrying biomolecular shuttles. Nanotechnology 2006;17:349–54.
[241] Svoboda K, Mitra PP, Block SM. Fluctuation analysis of motor protein movement and single enzyme kinetics. Proc Natl Acad Sci USA 1994;91:11782–6.
[242] Böhm KJ, Stracke R, Unger E. Speeding up kinesin-driven microtubule gliding in vitro by variation of cofactor composition and physicochemical parameters. Cell Biol Int 2000;24:335–41.
[243] Böhm KJ, Stracke R, Baum M, Zieren M, Unger E. Effect of temperature on kinesin-driven microtubule gliding and kinesin ATPase activity. FEBS Lett 2000;466:59–62.
[244] Kawaguchi K, Ishiwata S. Temperature dependence of force, velocity, and processivity of single kinesin molecules. Biochem Biophys Res Commun 2000;272:895–9.
[245] Kellermayer MSZ, Pollack GH. Rescue of in vitro actin motility halted at high ionic strength by reduction of ATP to submicromolar levels. Biochim BiophysActa Bioenergetics 1996;1277:107–14.
[246] Wang F, Chen L, Arcucci O, Harvey EV, Bowers B, Xu Y, et al. Effect of ADP and ionic strength on the kinetic and motile properties of recombinant mouse myosin V. J Biol Chem 2000;275:4329–35.
[247] Liang B, Chen Y, Wang CK, Luo ZX, Regnier M, Gordon AM, et al. Ca^{2+} regulation of rabbit skeletal muscle thin filament sliding: role of cross-bridge number. Biophys J 2003;85:1775–86.
[248] Kawai M, Kido T, Vogel M, Fink RHA, Ishiwata S. Temperature change does not affect force between regulated actin filaments and heavy meromyosin in single-molecule experiments. J Phys Lond 2006;574:877–87.
[249] Yokokawa R, Takeuchi S, Kon T, Nishiura M, Ohkura R, Sutoh K, et al. Hybrid nanotransport system by biomolecular linear motors. J Microelectromech Syst 2004;13:612–9.
[250] Yokokawa R, Takeuchi S, Kon T, Sutoh K, Fujita H. Control techniques of kinesin-driven beads in microfluidic devices. Microtechnology in medicine and biology. In: 3rd IEEE/EMBS special topic conference. 2005. p. 260–3.
[251] Wasylycia JR, Sapelnikova S, Jeong H, Dragoljic J, Marcus SL, Harrison DJ. Nano-biopower supplies for biomolecular motors: the use of metabolic pathway-based fuel generating systems in microfluidic devices. Lab Chip 2008;8:979–82.
[252] Tsuda Y, Mashimo T, Yoshiya I, Kaseda K, Harada Y, Yanagida T. Direct inhibition of the actomyosin motility by local anesthetics in vitro. Biophys J 1996;71:2733–41.
[253] Miyamoto Y, Muto E, Mashimo T, Iwane AH, Yoshiya I, Yanagida T. Direct inhibition of microtubule-based kinesin motility by local anesthetics. Biophys J 2000;78:940–9.
[254] Konishi K, Uyeda TQP, Kubo T. Genetic engineering of a Ca^{2+} dependent chemical switch into the linear biomotor kinesin. FEBS Lett 2006;580:3589–94.
[255] Greene AC, Trent AM, Bachand GD. Controlling kinesin motor proteins in nanoengineered systems through a metal-binding on/off switch. Biotechnol Bioeng 2008;101:478–86.
[256] Gast FU, Dittrich PS, Schwille P, Weigel M, Mertig M, Opitz J, et al. The microscopy cell (MicCell), a versatile modular flowthrough system for cell biology, biomaterial research, and nanotechnology. Microfluid Nanofluid 2006;2:21–36.
[257] Dujovne I, van den Heuvel M, Shen Y, de Graaff M, Dekker C. Velocity modulation of microtubules in electric fields. Nano Lett 2008;8:4217–20.
[258] Wu D, Tucker R, Hess H. Caged ATP: fuel for bionanodevices. IEEE Trans Adv Pack 2005;28:594–9.
[259] Nomura A, Uyeda TQP, Yumoto N, Tatsu Y. Photo-control of kinesin–microtubule motility using caged peptides derived from the kinesin C-terminus domain. Chem Commun 2006:3588–90.
[260] Kato H, Nishizaka T, Iga T, Kinosita Jr K, Ishiwata S. Imaging of thermal activation of actomyosin motors. Proc Natl Acad Sci USA 1999;96:9602–6.
[261] Kawaguchi K, Ishiwata S. Thermal activation of single kinesin molecules with temperature pulse microscopy. Cell Motil Cytoskeleton 2001;49:41–7.
[262] Mihajlovic G, Brunet NM, Trbovic J, Xiong P, von Molnar S, Chase PB. All-electrical switching and control mechanism for actomyosin-powered nanoactuators. Appl Phys Lett 2004;85:1060–2.
[263] Nath N, Chilkoti A. Creating "smart" surfaces using stimuli responsive polymers. Adv Mater 2002;14:1243–7.
[264] Ionov L, Stamm M, Diez S. Reversible switching of microtubule motility using thermoresponsive polymer surfaces. Nano Lett 2006;6:1982–7.
[265] Martin BD, Velea LM, Soto CM, Whitaker CM, Gaber BP, Ratna B. Reversible control of kinesin activity and microtubule gliding speeds by switching the doping states of a conducting polymer support. Nanotechnology 2007;18, 055103/1–7.
[266] van den Heuvel MGL, Butcher CT, Lemay SG, Diez S, Dekker C. Electrical docking of microtubules for kinesin-driven motility in nanostructures. Nano Lett 2005;5:235–41.
[267] Bull JL, Hunt AJ, Meyhofer E. A theoretical model of a molecular-motor-powered pump. Biomed Microdev 2005;7:21–33.
[268] Nicolau DV, Nicolau DV, Solana G, Hanson KL, Filipponi L, Wang LS, et al. Molecular motors-based micro- and nano-biocomputation devices. Microelectron Eng 2006;83:1582–8.
[269] Hess H, Howard J, Vogel V. A piconewton forcemeter assembled from microtubules and kinesins. Nano Lett 2002;2:1113–5.
[270] Hess H, Clemmens J, Howard J, Vogel V. Surface imaging by self-propelled nanoscale probes. Nano Lett 2002;2:113–6.
[271] Whitesides GM, Mathias JP, Seto CT. Molecular self-assembly and nanochemistry: a chemical strategy for the synthesis of nanostructures. Science 1991;254:1312–9.
[272] Rothemund PWK. Folding DNA to create nanoscale shapes and patterns. Nature 2006;440:297–302.
[273] Sailor MJ, Link JR. "Smart dust": nanostructured devices in a grain of sand. Chem Commun 2005:1375–83.

[274] Seetharam R, Wada Y, Ramachandran S, Hess H, Satir P. Long-term storage of bionanodevices by freezing and lyophilization. Lab Chip 2006;6:1239–42.
[275] Uppalapati M, Huang YM, Jackson TN, Hancock WO. Enhancing the stability of kinesin motors for microscale transport applications. Lab Chip 2008;8:358–61.
[276] Thompson DAW. On growth and form. Cambridge: Cambridge University Press; 1961.
[277] Vogel V. Reverse engineering: learning from proteins how to enhance the performance of synthetic nanosystems. MRS Bull 2002:972–8.
[278] Kay ER, Leigh DA, Zerbetto F. Synthetic molecular motors and mechanical machines. Angew Chem Int Ed 2007;46:72–191.
[279] Fennimore AM, Yuzvinsky TD, Han WQ, Fuhrer MS, Cumings J, Zettl A. Rotational actuators based on carbon nanotubes. Nature 2003;424:408–10.